Preprints (www.preprints.org) | NOT PEER-REVIEWED | Posted: 10 December 2019 doi:10.20944/preprints201912.0140.v1

Article

Surprising behaviour of the Wageningen B-screw Series polynomials

Stephan Helma [1]

[1] Stone Marine Propulsion (SMP) Ltd., SMM Business Park, Dock Road, CH41 1DT, UK; sh@smpropulsion.com

Abstract: Undoubtedly the Wageningen B-screw Series is the most widely used systematic propeller series. It is very popular to preselect propeller dimensions during the preliminary design stage, but often it is also used to merely select the final propeller. Over time the originally measured data sets were faired and scaled to a uniform Reynolds number (based on chord length and section advance speed) of $2 \cdot 10^6$ to increase the reliability of the series. With the advent of the computer polynomials for the thrust and torque values were calculated from the available data sets. The measured data are typically presented in the well-known open-water curves of thrust and torque coefficients K_T and K_Q versus the advance coefficient J. Changing the presentation from open-water diagrams to efficiency maps reveals some unsuspected and surprising behaviours, such as multiple optima when optimizing for efficiency or even no optimum at all for certain conditions. These artefacts get more pronounced at higher pitch to diameter ratios and low blade numbers. The present work builds upon the paper presented by the author at the AMT'17 [4] and smp'19 [5] conferences and now includes the extended efficiency maps, as suggested by Danckwardt, for all propellers of the Wageningen B-screw Series.

Keywords: Propeller; Wageningen B-screw Series; open-water characteristics; propeller efficiency map; Danckwardt diagram; optimum propeller

---

1. Introduction

The Wageningen B-screw Series dates back to 1936, when van Lammeren and van Aken started to publish the first results [6]. In the following years the series was systematically expanded to include more than 120 propellers. The measured data were presented in open-water diagrams showing the dimensionless thrust and torque coefficients, K_T and K_Q, and the open water efficiency η_o as functions of the also dimensionless advance coefficient J:

$$K_T = \frac{T}{\rho n^2 D^4}, \tag{1}$$

$$K_Q = \frac{Q}{\rho n^2 D^5} = \frac{P_P}{2\pi\rho n^3 D^5}, \tag{2}$$

$$\eta_o = \frac{J}{2\pi} \cdot \frac{K_T}{K_Q}, \text{ and} \tag{3}$$

$$J = \frac{v_a}{nD}, \tag{4}$$

where T = measured thrust; Q = measured torque; P_P = propeller power; ρ = water density; n = shaft speed (in s^{-1}); D = propeller diameter; and v_a = speed of advance. If not stated otherwise, all values are in SI base units.

All tested propellers had a diameter of 240 mm and hence different section chord lengths due to the variable blade area ratio. The propellers were tested in varying model basins of MARIN using diverse rate of revolutions resulting in considerably different Reynolds numbers for each propeller in the whole series. Oosterveld and van Oossanen engaged in the formidable tasks to scale all available

© 2019 by the author(s). Distributed under a Creative Commons CC BY license.

Preprints (www.preprints.org) | NOT PEER-REVIEWED | Posted: 10 December 2019 doi:10.20944/preprints201912.0140.v1

open-water data sets to a uniform Reynolds number of $2 \cdot 10^6$ and to calculate polynomials by multiple regressions analysis [8]. With the help of these polynomials it is possible to calculate the thrust and torque coefficients as functions of the advance coefficient J, the pitch to diameter ratio P/D, the expanded blade area ratio A_e/A_0 and the number of blades Z:

$$K_T = \sum C_{s,t,u,v} \cdot J^s \cdot (P/D)^t \cdot (A_e/A_0)^u \cdot Z^v \text{ and} \tag{5}$$
$$K_Q = \sum C_{s,t,u,v} \cdot J^s \cdot (P/D)^t \cdot (A_e/A_0)^u \cdot Z^v, \tag{6}$$

where $C_{s,t,u,v}$ = coefficient; and s, t, u, and v = whole-number exponents.

These polynomials are widely used in either selecting the optimum propeller or as a basis for further refinements. It is of utmost significance that these polynomials are consistent and accurate.

2. Time line of experimental results

As shown by Helma for the B4-70 propeller, the open-water characteristics have changed substantially over time [4], see Fig. 1. The effect on the widely used B_p–δ diagram was also outlined, see Fig. 2.

Preprints (www.preprints.org) | NOT PEER-REVIEWED | Posted: 10 December 2019 doi:10.20944/preprints201912.0140.v1

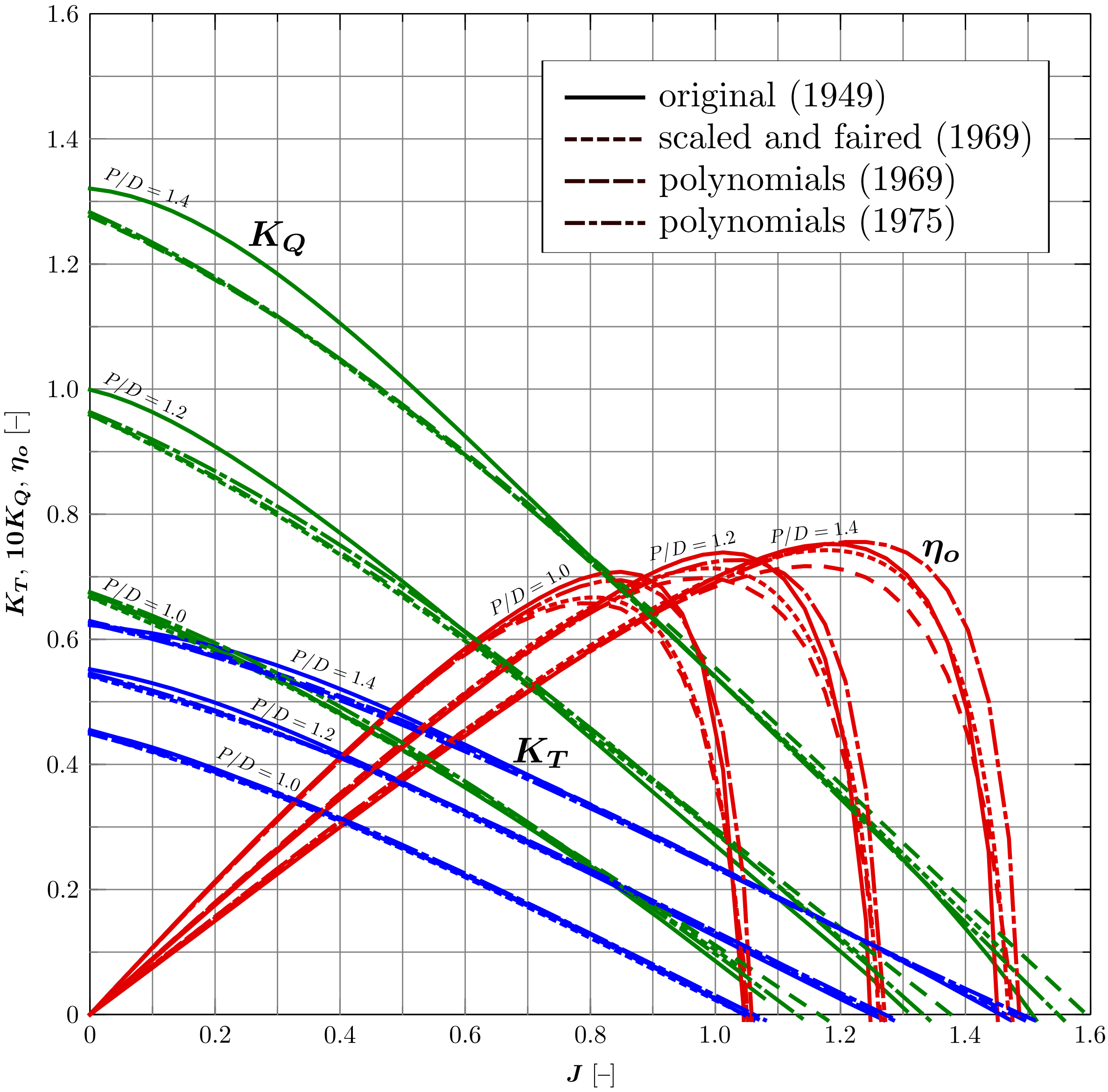

Figure 1. Originally measured by van Lammeren and van Aken in 1949 [6], the scaled and faired open-water characteristics, the fitted polynomials (both by van Lammeren *et al* in 1969 [7]), and the most recent polynomials by Oosterveld and van Oossanen in 1975 [8]) of propeller B4-70. The Reynolds number is $2.72 \cdot 10^5$ for the original data, otherwise $2 \cdot 10^6$. Reproduced from [4] with the permissions of the publisher.

Preprints (www.preprints.org) | NOT PEER-REVIEWED | Posted: 10 December 2019 doi:10.20944/preprints201912.0140.v1

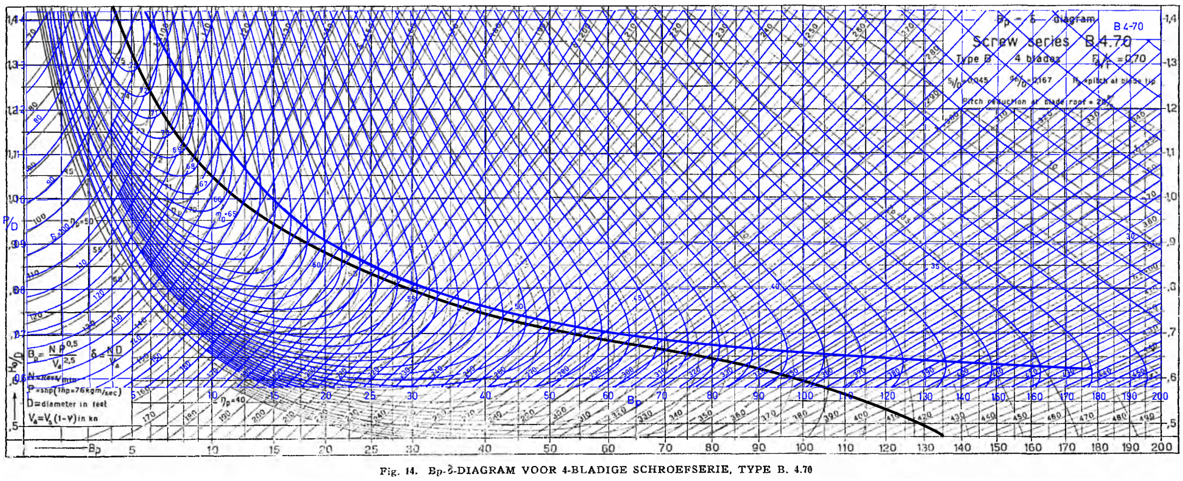

Figure 2. B_p–δ diagram of propeller B4-70 based on the originally measured values by van Lammeren and van Aken (1949) [6] [original print in black, Reynolds number = $2.72 \cdot 10^5$] and the scaled and faired open-water characteristics by van Lammeren *et al* (1969) [7] [blue, Reynolds number = $2 \cdot 10^6$]. Note the different bold lines showing the $\eta_{o,max}$ curve. $B_p = N \cdot \sqrt{P_D}/v_a^{2.5}$ and $\delta = N \cdot D/v_a$, where N = shaft speed (in min^{-1}); P_D = delivered power (in horsepower); v_a = speed of advance (in kn); and D = propeller diameter (in feet). Reproduced with the permissions of the publishers.

3. Efficiency maps

It is assumed, that the presentation in the form of the standard open-water diagrams for propellers are known to the reader. To recap, these diagrams show three families of curves with the thrust and torque coefficients and the efficiency as functions of the advance coefficient, $K_T(J)$, $K_Q(J)$ and $\eta_o(J)$, for a set of constant P/D-values for each propeller of the Wageningen B-screw Series.

Many authors suggested a different way of representing the non-dimensional open-water data (see Section 3.2); we will call them efficiency maps. On the K_Q–J efficiency map we draw the family of $K_Q(J)$ curves for our set of constant P/D-values as for the conventional open-water diagram (thin red lines, please refer to Figure 3). Instead of adding the family of efficiency curves for constant P/D-values, we add a family of parametric curves for the efficiency: $\eta_o\left(J, K_Q(J)\right) = \text{const}$ for a set of selected η_o-values (thin black lines). We can also draw the family of parametric curves for the thrust coefficient: $K_T\left(J, K_Q(J)\right) = \text{const}$ (dashed red lines). This gives us a diagram with the same information content as for the conventional open-water diagram, but displayed in a different way.

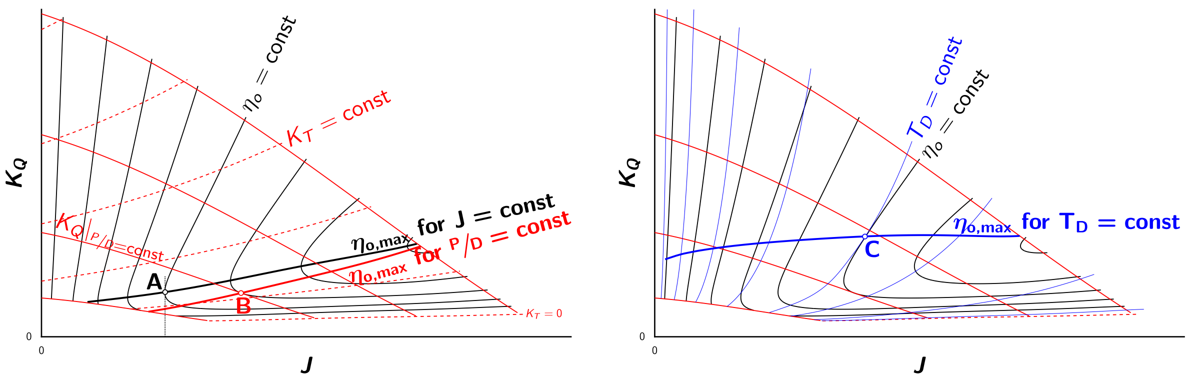

(a) Basic efficiency map showing K_Q (thin red lines), $K_T = \text{const}$ (dotted red lines), $\eta_o = \text{const}$ (thin black lines) and the construction of "$\eta_{o,max}$ for $J = \text{const}$" (dotted black line and point A, bold black line) and "$\eta_{o,max}$ for $P/D = \text{const}$" (point B, bold red line).

(b) Extended efficiency map additionally showing $T_D = \text{const}$ (thin blue lines) and the construction of "$\eta_{o,max}$ for $T_D = \text{const}$" (point C, bold blue line).

Figure 3. Composition of the K_Q–J efficiency map.

Preprints (www.preprints.org) | NOT PEER-REVIEWED | Posted: 10 December 2019 doi:10.20944/preprints201912.0140.v1

If the J-value is known, the propeller with the maximum efficiency can be found by drawing a vertical line at this given value of J (dotted black line). The propeller with the maximum efficiency can be found at the point where this vertical line just touches the efficiency curve (point A). The K_Q-value can be read off the ordinate and the K_T- and P/D-values can be interpolated. Connecting all points of these maximum efficiencies for every J-value results in the line "$\eta_{o,max}$ for $J = \text{const}$", which can be drawn into the efficiency map (bold black line). Note that the equivalent to this line on the conventional open-water diagram is the envelop to all $\eta_o(J)$ lines.

Another line of maximum efficiencies is the line called "$\eta_{o,max}$ for $P/D = \text{const}$" (bold red line). This line can be used to find the propeller with the maximum efficiency, if the P/D ratio is known. It connects all points, where the tangents of the K_Q and the η_o lines coincide (point B). On the conventional open-water diagram this line corresponds to the line connecting the maxima of all $\eta_o(J)$[1].

A second diagram, the K_T–J efficiency map, consists of $K_T(J)$ for the set of constant P/D-values and the parametric curves $K_Q\left(J, K_T(J)\right)$ and $\eta_o\left(J, K_T(J)\right) = \text{const}$ for the set of selected K_Q- and η_o-values. The lines for maximum efficiency are called "$\eta_{o,max}$ for $J = \text{const}$" and "$\eta_{o,max}$ for $P/D = \text{const}$" as before.

If the propeller diameter, the speed of advance and the (required) thrust are known, we can plot the curve

$$T_D(J) = \frac{K_T(J)}{J^2}, \tag{7}$$

which is equal to

$$T_D = \frac{1}{D^2 v_a^2} \frac{T}{\rho}, \tag{8}$$

into the efficiency map (thin blue lines). Note that this line can be drawn either in the K_T–J or in the K_Q–J efficiency map. In the K_T–J diagram, the line is a quadratic curve, whereas in the K_Q–J diagram, the line becomes the parametric curve

$$T_D\left(J, K_Q(J)\right) = \frac{K_T\left(J, K_Q(J)\right)}{J^2}. \tag{9}$$

In case of a given set of constant T_D-values, a family of curves results. Again a curve for propellers with the highest possible efficiency can be constructed; this is called the "$\eta_{o,max}$ for $T_D = \text{const}$" curve (thick blue line) by connecting the points where the tangent to the $T_D = \text{const}$ line coincides with the tangent to the $\eta_o = \text{const}$ curve (point C). We will see in Section 4.1, how this can be used to find the optimum propeller quickly, if the thrust T, the propeller diameter D and the speed of advance v_a is known.

Finally other families of curves for can be drawn for

$$P_D = \frac{K_Q}{J^3} = \frac{1}{D^2 v_a^2} \frac{Qn}{\rho v_a} = \frac{1}{D^2 v_a^2} \frac{P_P}{2\pi \rho v_a}, \tag{10}$$

$$T_n = \frac{K_T}{J^4} = \frac{n^2}{v_a^4} \frac{T}{\rho}, \text{ and} \tag{11}$$

$$P_n = \frac{K_Q}{J^5} = \frac{n^2}{v_a^4} \frac{Qn}{\rho v_a} = \frac{n}{v_a^4} \frac{P_P}{2\pi \rho v_a}. \tag{12}$$

The corresponding lines of maximum efficiency are called "$\eta_{o,max}$ for $P_D = \text{const}$", "$\eta_{o,max}$ for $T_n = \text{const}$" and "$\eta_{o,max}$ for $P_n = \text{const}$", respectively.

[1] Note, that this line is different from the envelope of all efficiency curves and gives a lower open-water efficiency.

Preprints (www.preprints.org) | NOT PEER-REVIEWED | Posted: 10 December 2019 doi:10.20944/preprints201912.0140.v1

3.1. Advantages

It was certainly noticed by the reader, that the efficiency maps introduced above are comparable, but not identical, to the B_p–δ diagram. One of the benefits of the efficiency maps is, that they include the bollard pull condition, whereas this condition disappears into infinity on the B_p–δ diagram, because δ as the inverse of the J-value, becomes infinity for $J = 0$.

The efficiency maps can also include lines with the solutions of four optimisation problems in one diagram[2], whereas one B_p–δ diagrams can only be used to solve one single problem. This is certainly another big advantage for the propeller designer.

3.2. Origins

The first diagrams using the presentation discussed in Section above were published in 1917 by Bendemann and Madelung[3] [2] and in 1923 by von der Steinen[4] [11]. Papmel published design charts in 1936 [9] using the same setup. Schoenherr included all four lines of maximum efficiency in 1949 [10]. All authors mentioned previously suggested to plot the T_D and T_n curves into the K_T–J efficiency map (and P_D and P_n into the K_Q–J efficiency map). Bendemann and Madelung pointed out, that the usage of a double logarithmic scale results in the T_D and T_n curves becoming straight lines, making it easier for the designer to use these maps. Danckwardt calculated design charts for the Wageningen B-screw Series in 1956 [3], but instead of drawing the T_D and T_n curves into the K_T–J efficiency map, he plotted the P_D and P_n curves (and *vice versa*. This deliberate decision makes life easier for the propeller designer (but not for the draftsman plotting these efficiency maps!), since now only one single chart is required to get also the missing torque or thrust coefficient. In 1983 Yosifov *et al* recalculated the design charts for the Wageningen B-screw Series with the aid of a computer using the polynomials [12], which became available in 1975 [8]. Finally Yosifov *et al* published polynomials for the $\eta_{o,max}$ lines in 1986 [13].

All these diagrams might use different symbols or alternative definitions of the variables (mostly multiplied by constant values or using inverse values) and show different degrees of details, but they all build on the idea of the efficiency map. Examples for Danckwardt diagrams and diagrams calculated by Yosifov *et al* are shown in Figures 4–5 and 6–7, respectively.

4. Danckwardt's efficiency maps

As mentioned in Section 3.2, unlike all other authors, Danckwardt used the P_D and P_n curves in the K_T–J efficiency map. This innovation allows the propeller designer to read all values off one single diagram. An overview of the composition of these diagrams is given in Table A1 and an example how these diagrams are used, is explained in Section 4.1.

To honour the inventor, this set of efficiency maps came to be known as Danckwardt diagrams. As the originator, we will call them the T–J and P–J diagrams to distinguish them from the general efficiency maps K_T–J and K_Q–J. As a mnemonic use the T–J diagram whenever the thrust T is known and P–J whenever the power P_D or the torque Q is known.

---

2 It is possible to include the lines for all six optimisation problems in one diagram, but then this diagram would become even more confusing.

3 They based their idea how the data should be presented on the polar diagram of aerofoils, which is also known as Lilienthal diagram.

4 Von der Steinen argues, that he has finished his paper earlier, but could not publish it for 6 years because of a exceptionally high work load, thus claiming the intellectual property [11].

Preprints (www.preprints.org) | NOT PEER-REVIEWED | Posted: 10 December 2019 doi:10.20944/preprints201912.0140.v1

Table 1. Differences between the nomenclature used by Danckwardt and ITTC.

Name	Danckwardt	ITTC
Pitch	H	P
Blade area ratio	F_a/F	A_e/A_0
Speed of advance	v_e	v_a
Thrust	S	T
Torque	M	Q
Delivered power	N_W	P_D
Advance coefficient	Λ	J
Thrust coefficient	k_s	K_T
Torque coefficient	k_m	K_Q
Open-water efficiency	η_P	η_o
Slip	s_n	S_R

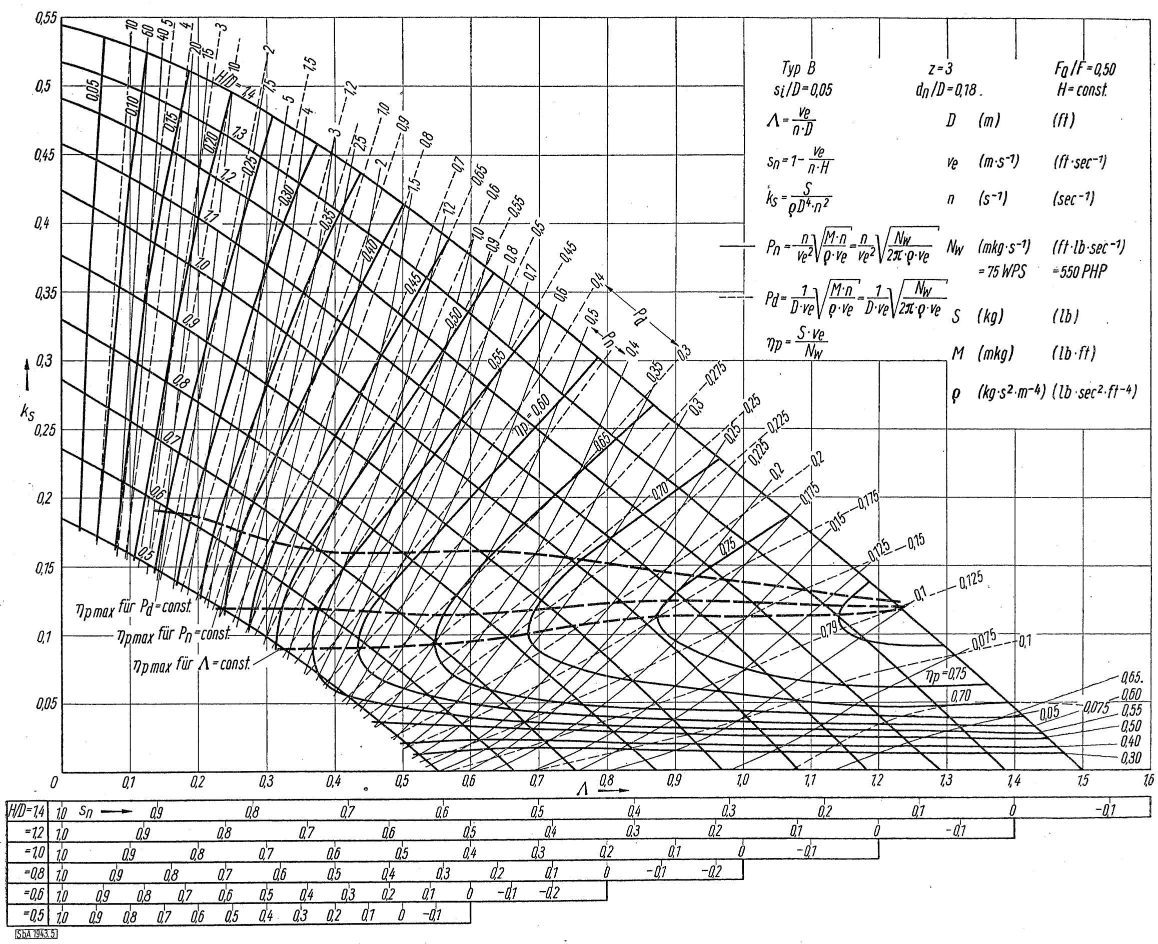

Bild 36. N_w–Λ-Diagramm B 3.50

(Entnommen aus „Schiffbautechnik“ Heft 2/56, Seite 27, VEB Verlag Technik, Berlin)

Figure 4. Example of an original Danckwardt T–J diagram for the propeller B3-50 [3]. It is based on the K_T–J efficiency map and Danckwardt called it the N_w–Λ diagram. (See also Table 1 for the differences between Danckwardt's and ITTC's nomenclature.)

Preprints (www.preprints.org) | NOT PEER-REVIEWED | Posted: 10 December 2019 doi:10.20944/preprints201912.0140.v1

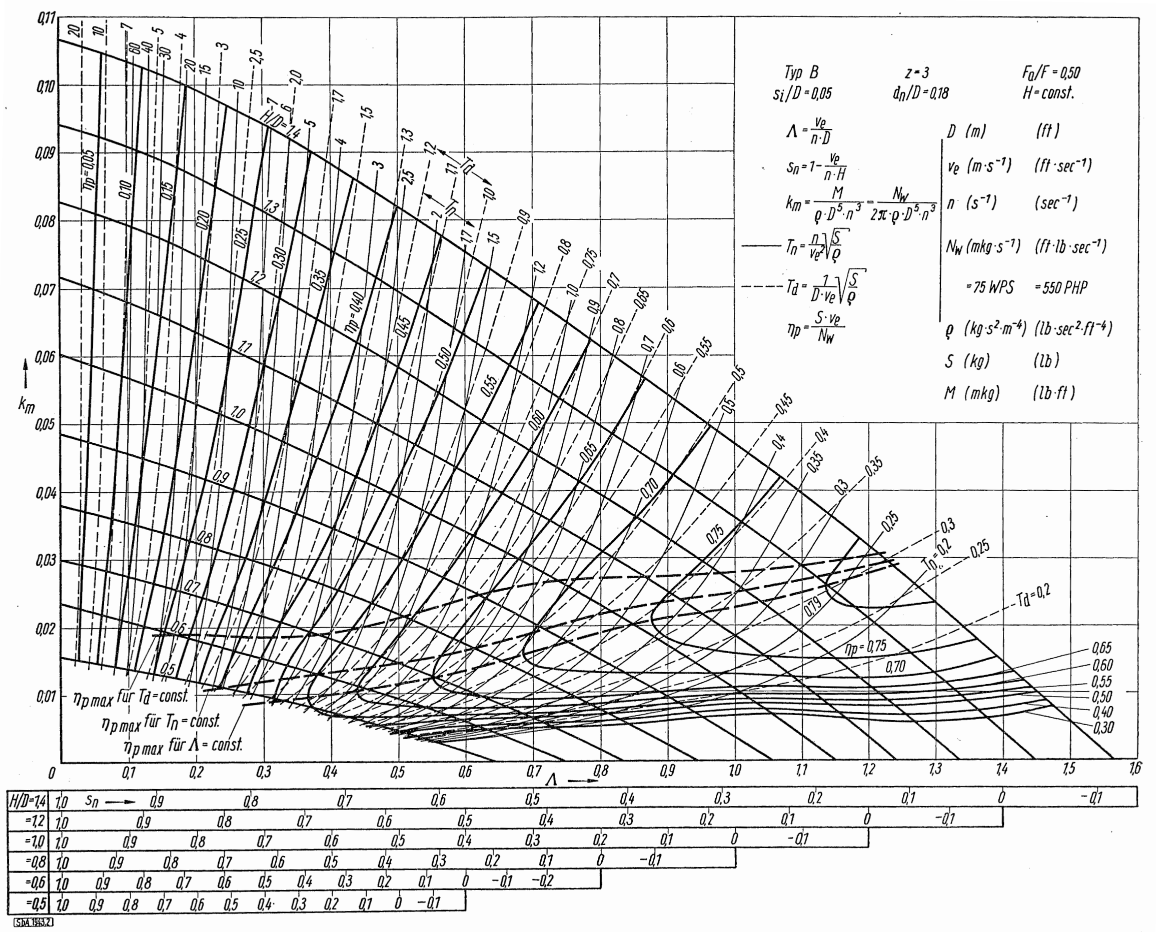

Bild 35. s–Λ-Diagramm B 3.50

(Entnommen aus „Schiffbautechnik" Heft 2/56, Seite 23. VEB Verlag Technik, Berlin)

Figure 5. Example of an original Danckwardt P–J diagram for the propeller B3-50 [3]. It is based on the K_Q–J efficiency map and Danckwardt called it the s–Λ diagram. (See also Table 1 for the differences between Danckwardt's and ITTC's nomenclature.)

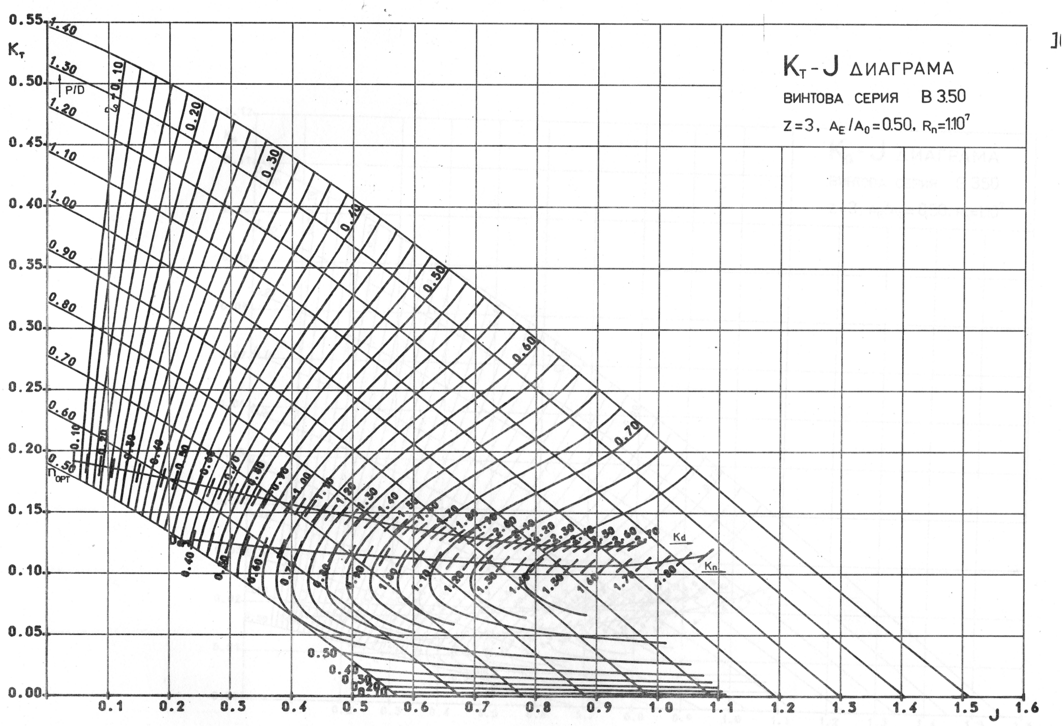

Figure 6. Example of a Papmel K_T–J efficiency map for the propeller B3-50 as recreated by Yosifov *et al* [13]. Note the use of $K_d = 1/\sqrt{T_D}$ and $K_n = 1/\sqrt[4]{T_n}$.

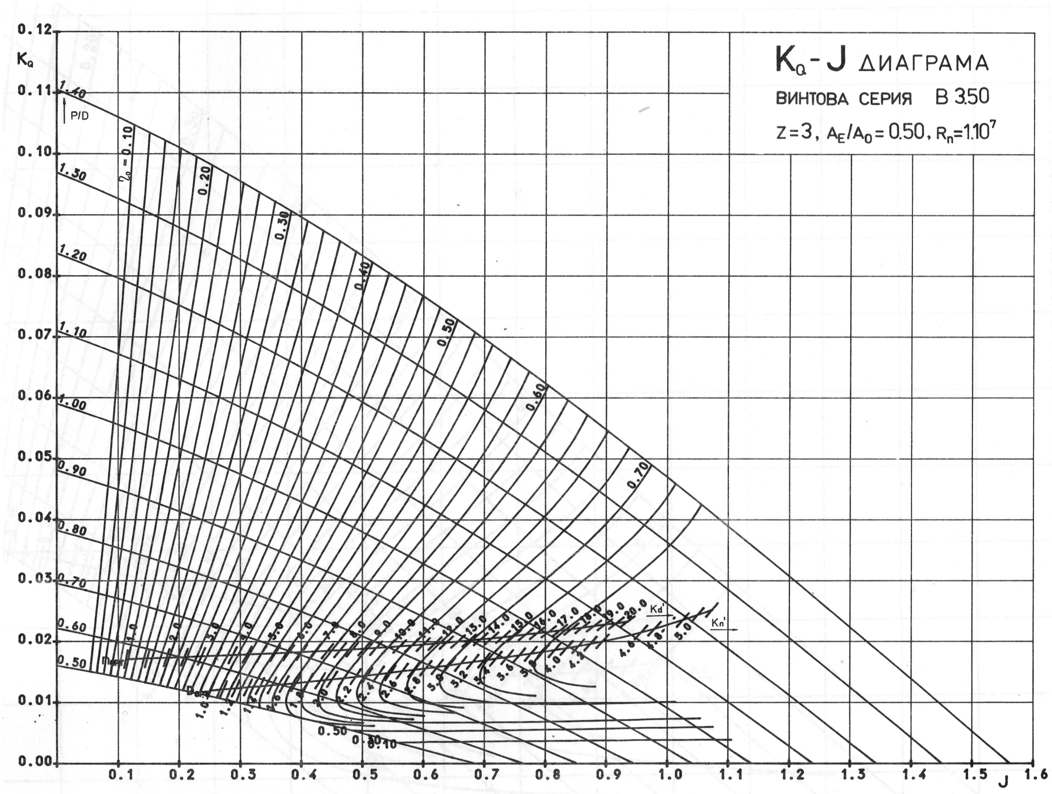

Figure 7. Example of a Papmel K_Q–J efficiency map for the propeller B3-50 as recreated by Yosifov *et al* [13]. Note the use of $K'_d = 3.455/\sqrt{P_D}$ and $K'_n = 3.455/\sqrt[4]{P_n}$.

Preprints (www.preprints.org) | NOT PEER-REVIEWED | Posted: 10 December 2019 doi:10.20944/preprints201912.0140.v1

4.1. Usage

The Danckwardt diagrams can be used to find the optimum propeller. For the sake of argument let us assume that we know the available torque Q, the inflow velocity v_a and the shaft speed n. Using these values we can calculate P_n from equation (12). Let us further assume that the computed value for P_n is 0.5 and we want to work out the optimum pitch, diameter and required torque for a propeller with 5 blades and a blade area ratio of 0.9. On the Danckwardt P–J chart for the Wageningen B5-90 propeller (see Appendix), we find the intersection of the line for $P_n = 0.5$ with the "$\eta_{o,max}$ for $P_n = \text{const}$" curve (green lines). We can read off the values for J, K_T, K_Q, P/D, and η_o (approximately 0.60, 0.24, 0.040, 1.0, and 0.57, respectively). From J we can calculate the diameter and once D is known, we can calculate the thrust and pitch from K_Q and P/D. If we were thus inclined, we can transfer the optimized propeller into the Danckwardt T–J diagram and cross-check the result.

4.2. Remake

For this paper, the two Danckwardt diagrams for all propellers of the Wageningen B-screw Series as outlined in Table 2 were re-created with the help of a purpose-made computer program. This program employs the polynomials (5) and (6) as described in Section 1 and published by Oosterveld and van Oossanen in 1975 [8]. For these newly generated diagrams the symbols were updated to the ITTC nomenclature [1] (see also Table 1 for the differences to the nomenclature used by Danckwardt). In addition to the curves presented in the original diagrams, the line showing "$\eta_{o,max}$ for $P/D = \text{const}$" and the family of curves $K_T(J, K_Q)$ or $K_Q(J, K_T) = \text{const}$ were added. All these recalculated Danckwardt diagrams are presented in the Appendix A.

Table 2. Summary of the Wageningen B-screw Series.

Z	A_e/A_0																
2	0.30		0.38														
3		0.35				0.50			0.65			0.80					
4				0.40			0.55			0.70			0.85			1.00	
5					0.45			0.60			0.75			0.90			1.05
6						0.50			0.65			0.80			0.95		
7							0.55			0.70			0.85				

It must be mentioned, that the calculation of the $\eta_{o,max}$ curves for T_D, T_n, P_D, and $P_n = \text{const}$ sometimes did not succeed at one or the other boundary due to numerical difficulties. The artefacts on the left boundary at low J- and P/D-values were manually deleted and extrapolated by hand whenever possible. The right border, where the J- and P/D-values are high, posed a different challenge. In all cases it was however possible to reconstruct the valid line manually, but sometimes not right up to the maximum P/D. It should be mentioned, that this problem never arose when the $\eta_{o,max}$ curves doubles back as discussed in the following section.

5. Ambiguity of the $\eta_{o,max}$ curves

We have seen in section 3.2, how an optimum propeller can be worked out with a minimum of effort. Let us now assume, that we want to investigate a three bladed propeller with a blade area ratio A_e/A_0 of 0.80 (Wageningen B3-80 propeller). For our presumed value of 0.5 for P_n, we find the intersection with the "$\eta_{o,max}$ for $P_n = \text{const}$" curve (green lines) at J, K_T, K_Q, P/D, and η_o equal to 0.59, 0.21, 0.035, 0.98, and 0.56, respectively. But there also exists another intersection between the $P_n = 0.5$ and the "$\eta_{o,max}$ for $P_n = \text{const}$" lines at a higher P/D-value: 0.69, 0.35, 0.075, 1.35, and 0.51. This clearly indicates that there are two optimum propellers for this condition!

The reason for this somewhat puzzling behaviour is obviously the doubling back of the $\eta_{o,max}$ curves. This only ever happens for the T_D, T_n, P_D and P_n curves, but never for "$\eta_{o,max}$ for $J = \text{const}$" or "$\eta_{o,max}$ for $P/D = \text{const}$". To classify the overlap, the value of T_D, where the "$\eta_{o,max}$ for $T_D = \text{const}$"

Preprints (www.preprints.org) | NOT PEER-REVIEWED | Posted: 10 December 2019 doi:10.20944/preprints201912.0140.v1

curve intersects the maximum $P/D|_{\max}$ line ($T_D|_{P/D|_{\max}}$) was calculated for each propeller (please refer to Figure 8). Then the intersection of this T_D = const line with the "$\eta_{o,max}$ for T_D = const" curve was found. The pitch to diameter ratio at this intersection is denoted as $\widehat{P/D}|_{T_D}$. The minimum value of $T_D|_{\min}$ is determined, too. There is no optimum propeller right of this minimum value! The difference between these two values for T_D is denoted ΔT_D. For the T_n, P_D, and P_n curves, these values are calculated accordingly. The Table 3 shows an overview of these values for all propellers of the Wageningen B-screw Series.

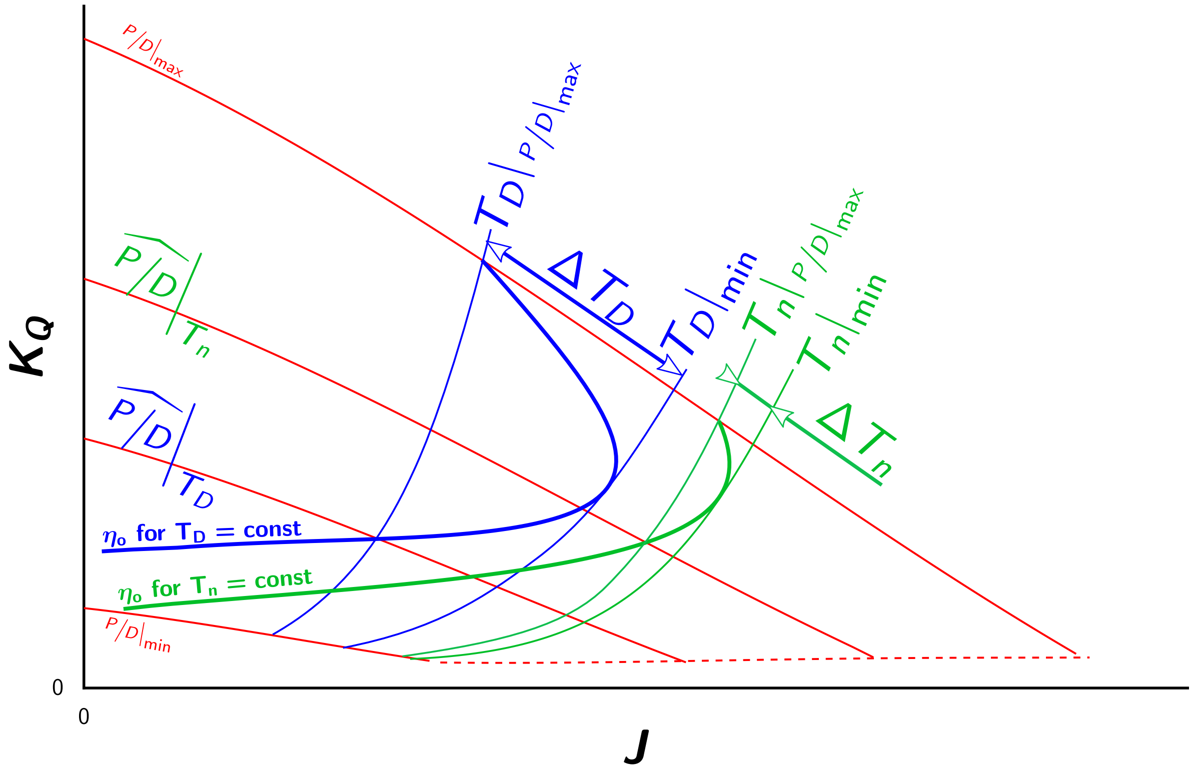

Figure 8. Symbols and definitions used to describe the overlap of the $\eta_{o,max}$ curves given in Table 3 using the example of the T_D and T_n curves in the Danckwardt T–J efficiency map.

Table 3. Main characteristics of the overlaps found in the re-created Danckwardt diagrams. (For symbols and definitions see Section 5 and Figure 8.)

	T_D			T_n			P_D			P_n		
Propeller	$\widehat{P/D}$	$T_D\vert_{\min}$	ΔT_D	$\widehat{P/D}$	$T_n\vert_{\min}$	ΔT_n	$\widehat{P/D}$	$P_D\vert_{\min}$	ΔP_D	$\widehat{P/D}$	$P_n\vert_{\min}$	ΔP_n
B2-30		———			———			———			———	
B2-38		———			———			———			———	
B3-35	0.95	0.39	0.187	1.15	0.32	0.061	0.94	0.18	0.104	1.15	0.15	0.030
B3-50	0.90	0.41	0.218	1.14	0.34	0.057	0.89	0.19	0.127	1.13	0.16	0.029
B3-65	0.87	0.48	0.305	1.13	0.40	0.064	0.87	0.23	0.193	1.12	0.19	0.034
B3-80	0.87	0.62	0.527	1.12	0.52	0.084	0.86	0.32	0.383	1.12	0.25	0.046
B4-40	1.03	0.52	0.115	1.18	0.42	0.047	1.02	0.25	0.068	1.18	0.20	0.024
B4-55	1.05	0.48	0.095	1.24	0.38	0.023	1.04	0.23	0.054	1.23	0.18	0.012
B4-70	1.11	0.48	0.063	1.32	0.37	0.005	1.11	0.23	0.036	1.32	0.17	0.003
B4-85	1.22	0.50	0.026		———		1.22	0.24	0.015		———	
B4-100		———			———			———			———	
B5-45	1.22	0.55	0.025	1.30	0.44	0.009	1.22	0.27	0.014	1.30	0.21	0.005
B5-60	1.26	0.48	0.016	1.36	0.38	0.002	1.26	0.23	0.009	1.36	0.18	0.001
B5-75	1.33	0.44	0.004		———		1.33	0.21	0.002		———	
B5-90		———			———			———			———	
B5-105		———			———			———			———	
B6-50	1.37	0.50	0.001		———		1.37	0.24	0.001		———	
B6-65	1.38	0.46	0.001		———		1.37	0.22	0.001		———	
B6-80		———			———			———			———	
B6-95		———			———			———			———	
B7-55		———			———			———			———	
B7-70		———			———			———			———	
B7-85		———			———			———			———	

It must be mentioned, that these overlaps are not a feature of the presentation in the form of the efficiency map but of the underlying data, i.e. the polynomials (5) and (6) published by Oosterveld & van Oossanen [8]. It should be noted that at the time when Danckwardt published his diagrams – which show no overlaps at all – the polynomials were not known yet. The efficiency maps published by Yosifov *et al* are already based on the polynomials [13]. On all of their efficiency maps, the curves for $\eta_{o,max}$ stop before they reach the maximum P/D-value. Yosifov *et al* do not mention this behaviour. Those diagrams where the lines stop far from the maximum P/D ratio are for the same propellers, where we have identified an overlap.

It is expected that any automatic optimization routine based on these polynomials eventually will encounter the problem of a double optima and might ultimately fail or give a random value, if no precautionary measures are taken.

The author of this paper believes that these overlaps of the $\eta_{o,max}$ curves are physically not explainable.

To support this view, let us assume that we extend the propeller series to even higher P/D-values. Eventually we will arrive at a pitch setting, where the open-water efficiency will become zero, since such a propeller would have blades perpendicular to the section inflow and hence would not be able to accelerate water in the axial direction. Thus it is not unreasonable to assume that a pitch to diameter ratio must exist, where the open-water efficiency is globally at its highest. And indeed this can be seen in both Danckwardt diagrams for the Wageningen B2-30 and B2-38 propeller (see Appendix A): A peak of the open-water efficiency can be noticed at a J-value of about 1 and a P/D ratio of about 1.1. It can be observed that all four curves for $\eta_{o,max}$ passes (and must pass) through this absolute maximum of η_o. Even if this point of the absolute maximum of η_o comes to lie right of and above the set of K_T and K_Q curves, the four curves for $\eta_{o,max}$ must still converge towards this single point of the absolute

Preprints (www.preprints.org) | NOT PEER-REVIEWED | Posted: 10 December 2019 doi:10.20944/preprints201912.0140.v1

maximum of η_o. Following this thought it is obvious that the lines of $\eta_{o,max}$ can not bend back as can be seen with certain propellers and this behaviour is deemed as physically inexplicable.

6. Conclusion

With the help of the alternative presentation of open-water characteristics as efficiency maps it was shown that the current set of polynomials for the Wageningen B-screw Series as published by Oosterveld & van Oossanen in 1975 [8] shows some troublesome behaviours for higher pitch to diameter ratios for many propellers of the series. At the moment, the source of this behaviour is not known, but some possibilities spring to mind: Between the testing of the first and the last propeller, a time span of more than 30 years passed. During this timespan it can be assumed that the manufacturing of the model propellers and the testing technology improved. The propellers were tested at different basins and also at different Reynolds numbers and were only later corrected to a uniform Reynolds number of $2 \cdot 10^6$. Even the numerical regression used to calculate the polynomials could have introduced this behaviour.

Considering the widespread use of these polynomials, it is suggested to revisit the originally tested data and check all steps involved in the processing of the data sets for the deduction of the polynomials.

The propeller designers would be well advised to take caution when designing propellers whenever any curve of $\eta_{o,max}$ doubles back.

Funding: This research received no external funding.

Conflicts of Interest: The author declares no conflict of interest.

Abbreviations

The following abbreviations are used in this manuscript:

AMT	International Conference on Advanced Model Measurement Technology for the Maritime Industry
ITTC	International Towing Tank Conference
MARIN	Maritime Research Institute Netherlands
smp	International Symposium on Marine Propulsors

Appendix A

The following pages contain the re-created Danckwardt diagrams of all propellers of the Wageningen B-screw Series according to Table 2. They are valid for a sectional Reynolds number of $2 \cdot 10^6$. The diagrams are based on the polynomials published in 1975 by Oosterveld & van Oossanen [8]. The Table A1 explains the composition of the diagrams and the line colours and types used.

Table A1. Composition of the Danckwardt P–J (K_T–J) and T–J (K_Q–J) efficiency maps. Also shown is the significations of line colour and type. K_T = thrust coefficient; K_Q = torque coefficient; η_o = open-water efficiency; J = advance coefficient; T = thrust; Q = torque; P_P = propeller power; D = propeller diameter; P = propeller pitch; n = shaft speed (in s^{-1}); v_a = speed of advance; and ρ = water density. If not stated otherwise, all values are in SI base units.

Diagram:	**P–J**	**T–J**
Abscissa:	$\boldsymbol{J} = \frac{v_a}{nD}$	$\boldsymbol{J} = \frac{v_a}{nD}$
Ordinate:	$\boldsymbol{K_T} = \frac{T}{\rho n^2 D^4}$	$\boldsymbol{K_Q} = \frac{Q}{\rho n^2 D^5} = \frac{P_P}{2\pi\rho n^3 D^5}$
One set of curves:	$K_T(J)$ for $P/D = \text{const}$	$K_Q(J)$ for $P/D = \text{const}$
Four families of parametric curves for sets of constant values:	$\eta_o = \frac{v_a}{nD} = \text{const}$	$\eta_o = \frac{v_a}{nD} = \text{const}$
	$K_Q = \frac{Q}{\rho n^2 D^5} = \frac{P_P}{2\pi\rho n^3 D^5} = \text{const}$	$K_T = \frac{T}{\rho n^2 D^4} = \text{const}$
	$P_D = \frac{K_Q}{J^3} = \frac{1}{D^2 v_a^2}\frac{Qn}{\rho v_a} = \frac{1}{D^2 v_a^2}\frac{P_P}{2\pi\rho v_a} = \text{const}$	$T_D = \frac{K_T}{J^2} = \frac{1}{D^2 v_a^2}\frac{T}{\rho} = \text{const}$
	$P_n = \frac{K_Q}{J^5} = \frac{n}{v_a^4}\frac{Qn}{\rho v_a} = \frac{n}{v_a^4}\frac{P_P}{2\pi\rho v_a} = \text{const}$	$T_n = \frac{K_T}{J^4} = \frac{n}{v_a^4}\frac{T}{\rho} = \text{const}$
Four curves of $\eta_{o,max}$:	"for $\boldsymbol{P_D}$**= const**" (for known Q, v_a, D)	"for $\boldsymbol{T_D}$**= const**" (for known T, v_a, D)
	"for $\boldsymbol{P_n}$**= const**" (for known Q, v_a, n)	"for $\boldsymbol{T_n}$**= const**" (for known T, v_a, n)
	"for $\boldsymbol{J}$**= const**" (for known v_a, n, D)	"for $\boldsymbol{J}$**= const**" (for known v_a, n, D)
	"for **P/D= const**" (for known P/D)	"for **P/D= const**" (for known P/D)

Preprints (www.preprints.org) | NOT PEER-REVIEWED | Posted: 10 December 2019
doi:10.20944/preprints201912.0140.v1

Preprints (www.preprints.org) | NOT PEER-REVIEWED | Posted: 10 December 2019

doi:10.20944/preprints201912.0140.v1

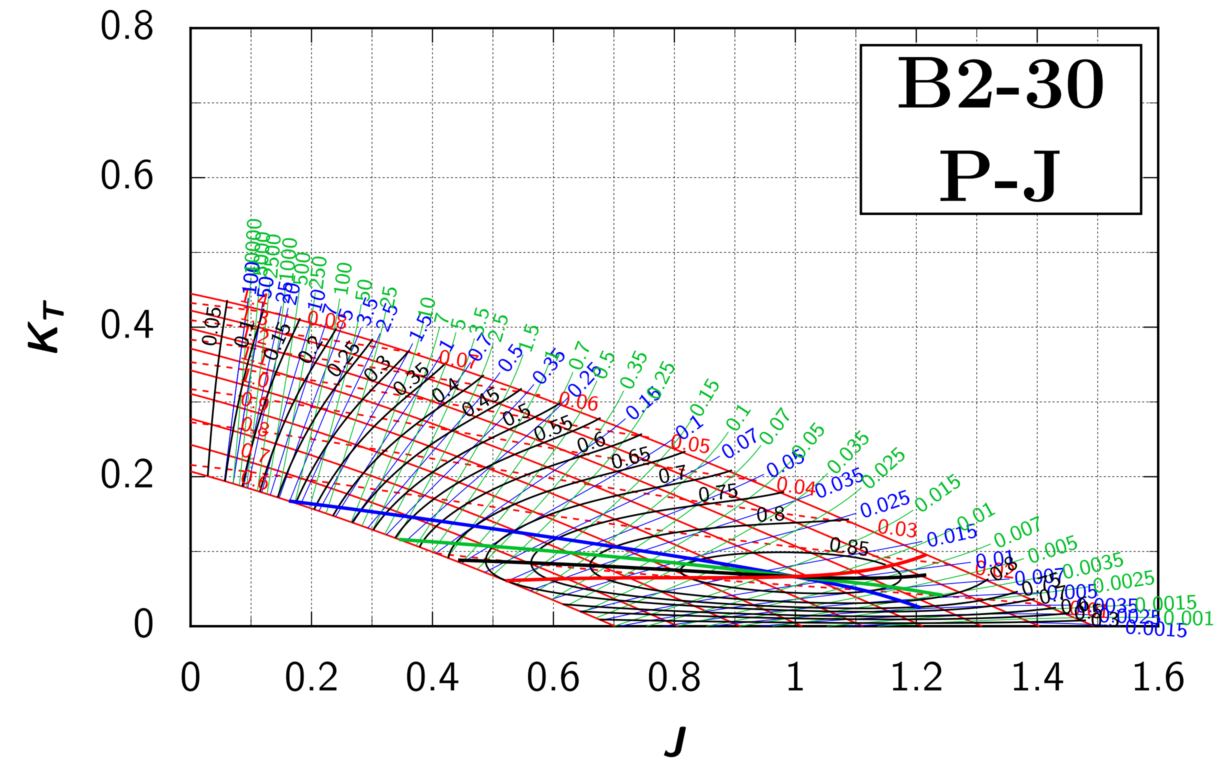
B2-30
P-J
K_T
J
0
0.2
0.4
0.6
0.8
1
1.2
1.4
1.6

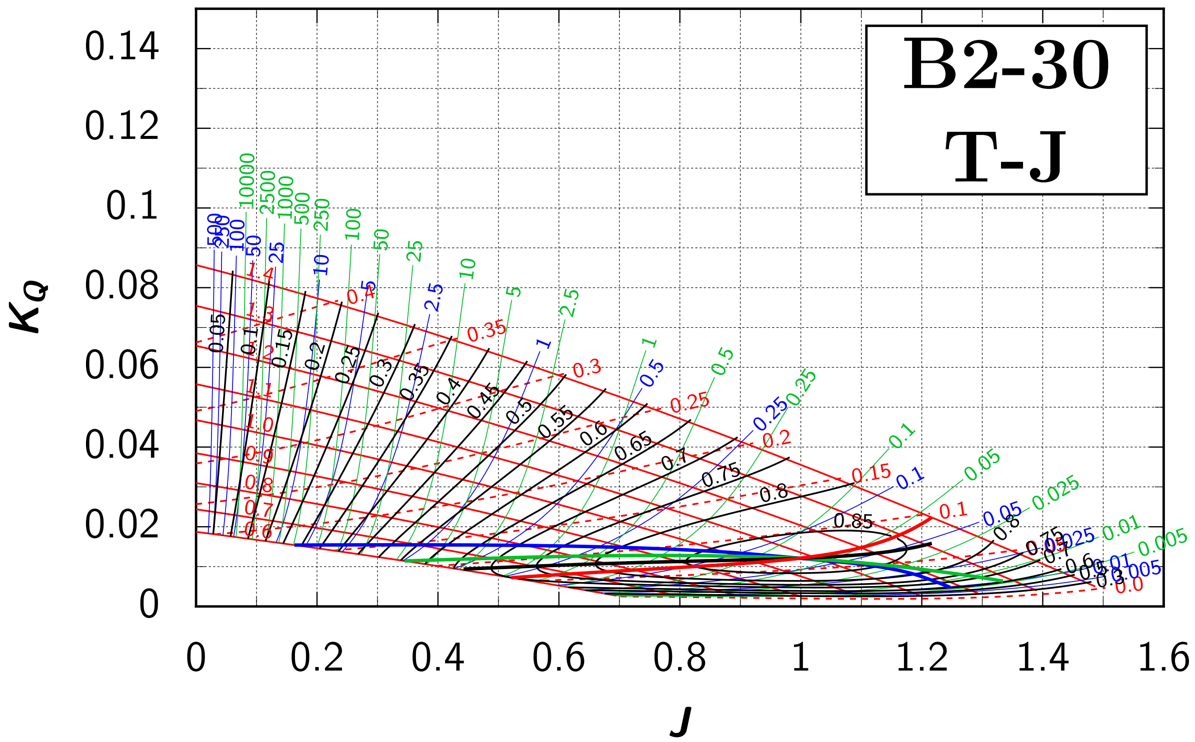
B2-30
T-J
K_Q
J
0
0.02
0.04
0.06
0.08
0.1
0.12
0.14
0.2
0.4
0.6
0.8
1
1.2
1.4
1.6

Preprints (www.preprints.org) | NOT PEER-REVIEWED | Posted: 10 December 2019 doi:10.20944/preprints201912.0140.v1

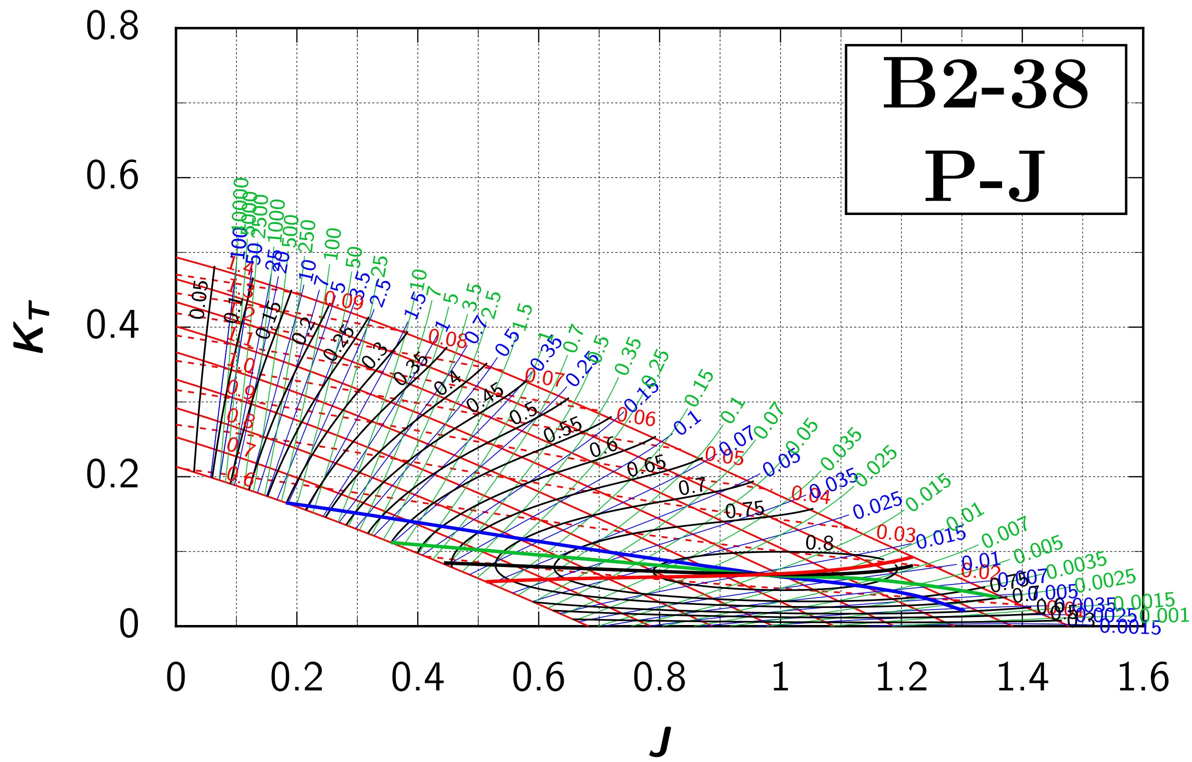

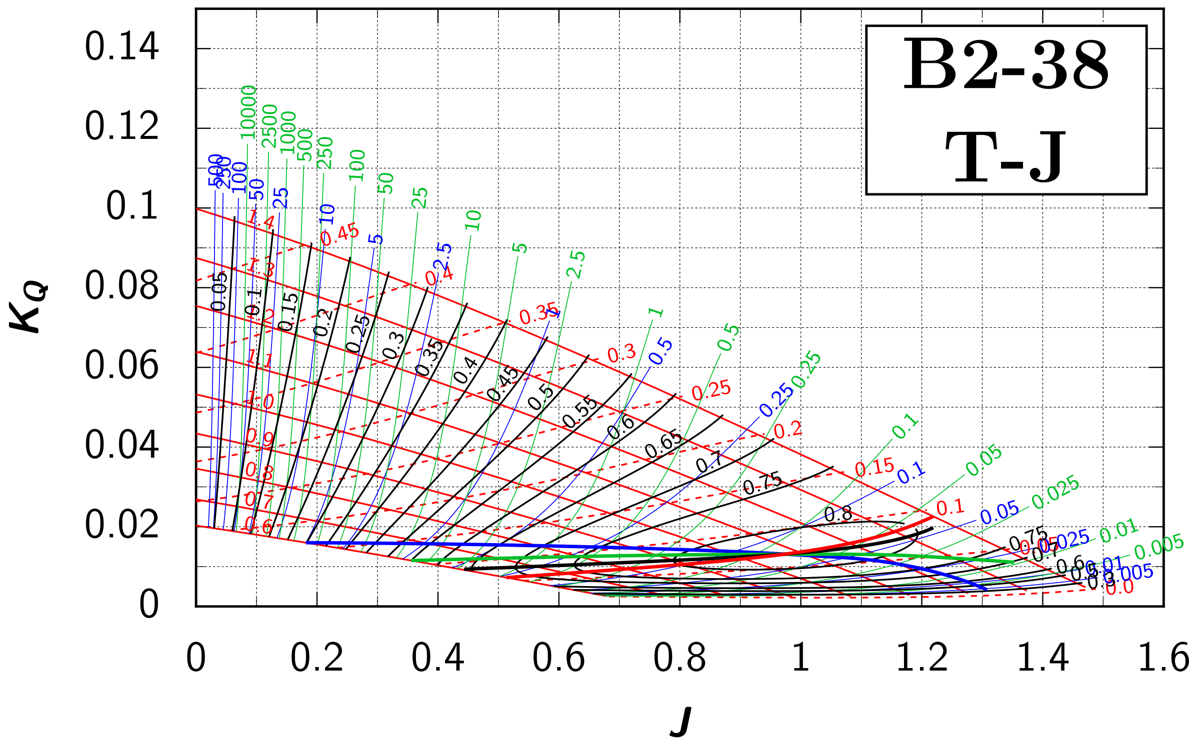

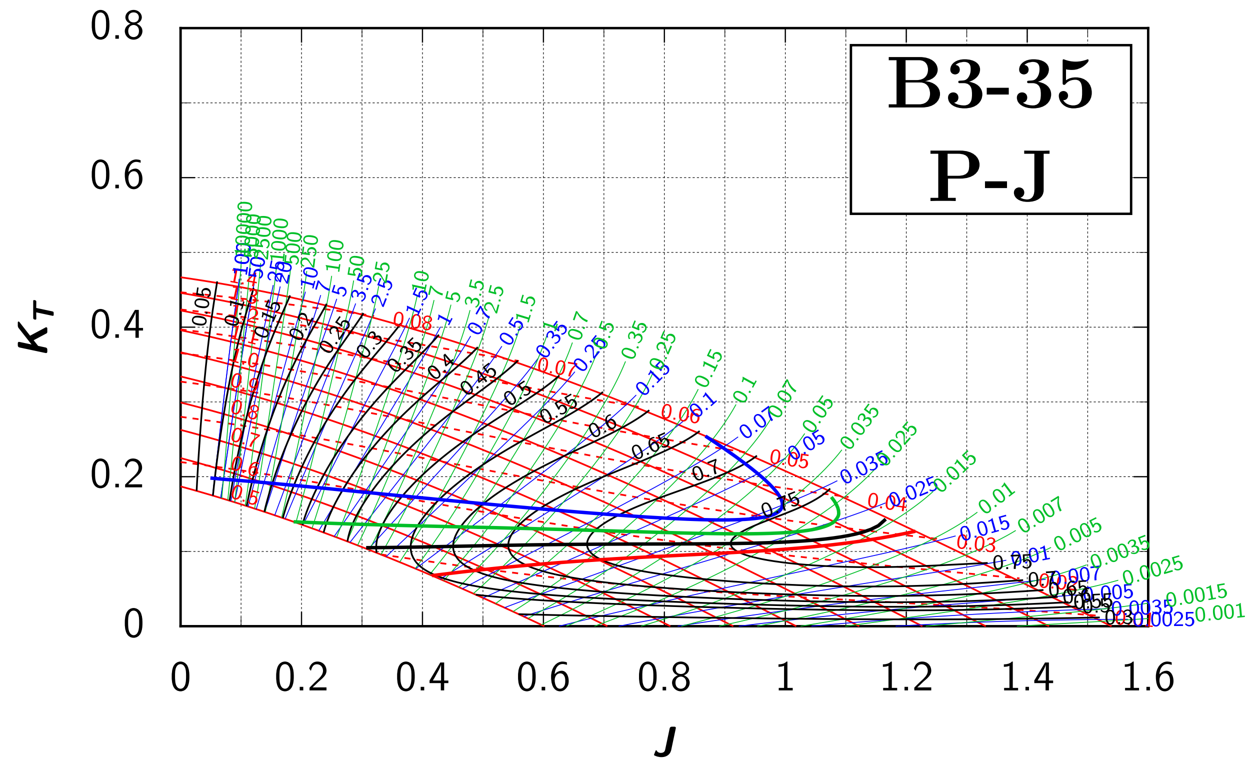
B3-35
P-J
K_T
J
0
0.2
0.4
0.6
0.8
1
1.2
1.4
1.6

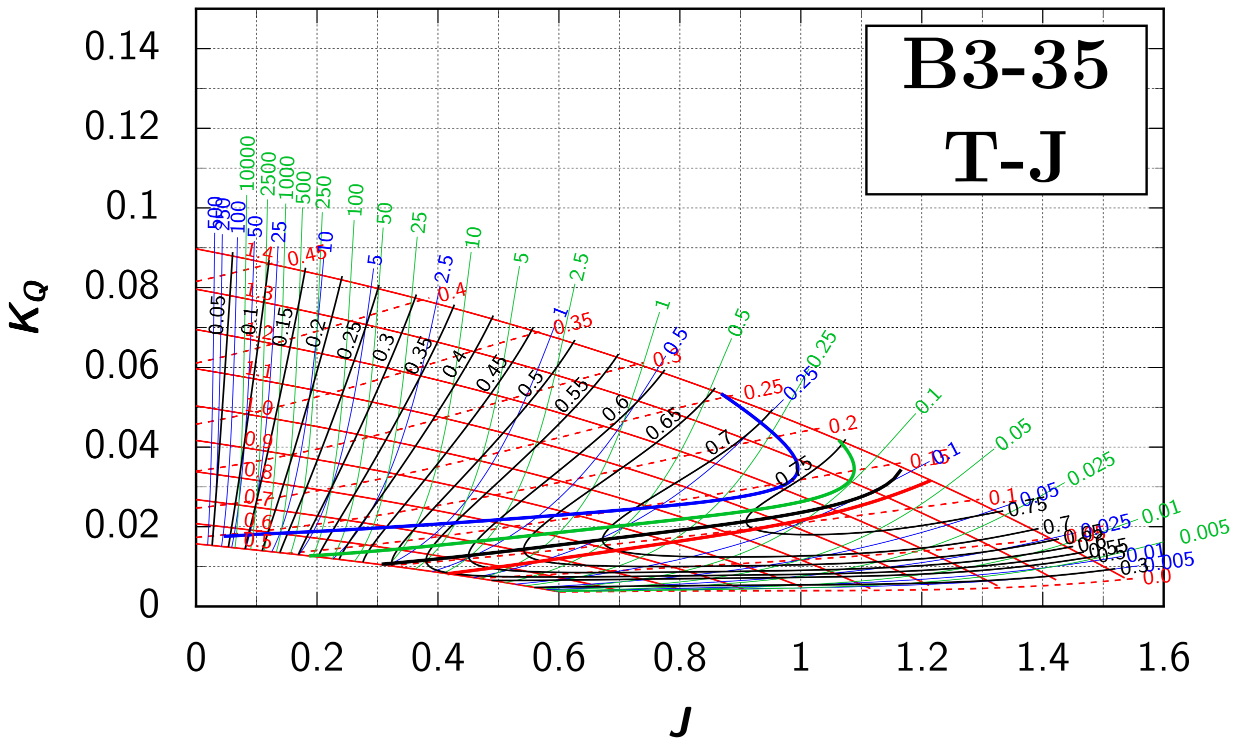
B3-35
T-J
K_Q
J
0
0.02
0.04
0.06
0.08
0.1
0.12
0.14
0.2
0.4
0.6
0.8
1
1.2
1.4
1.6

Preprints (www.preprints.org) | NOT PEER-REVIEWED | Posted: 10 December 2019 doi:10.20944/preprints201912.0140.v1

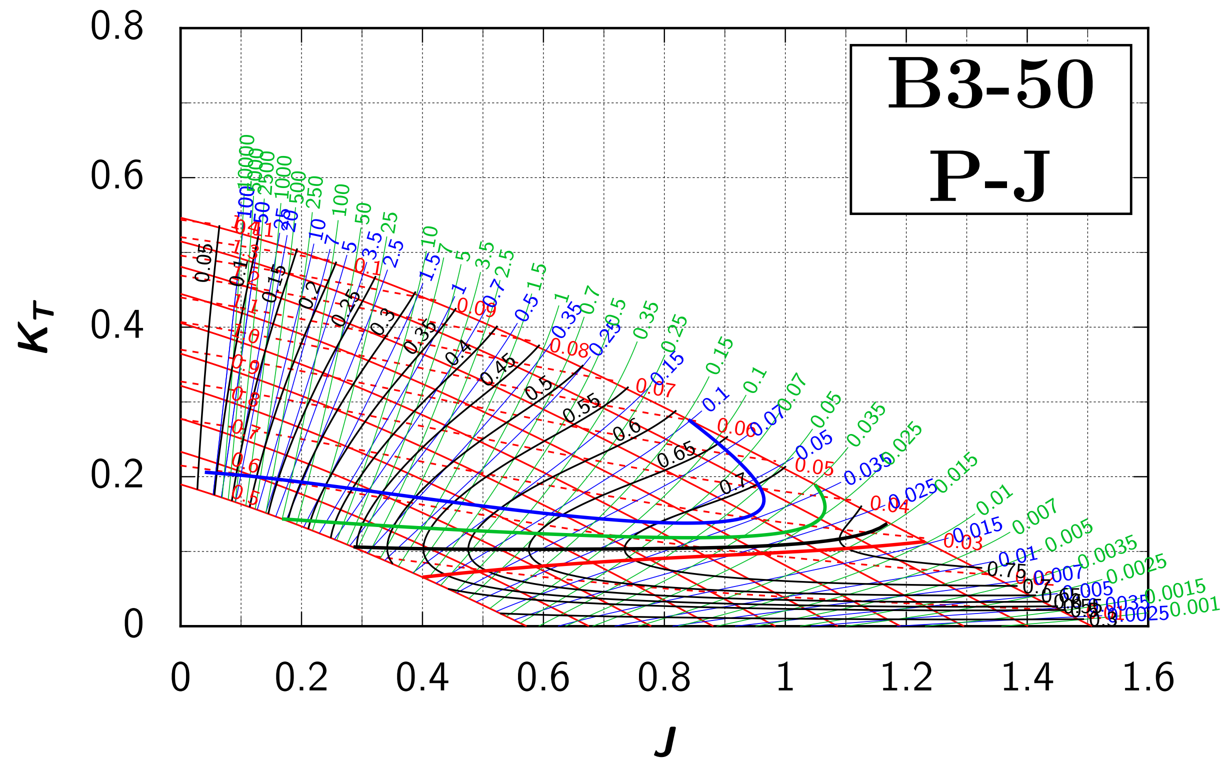

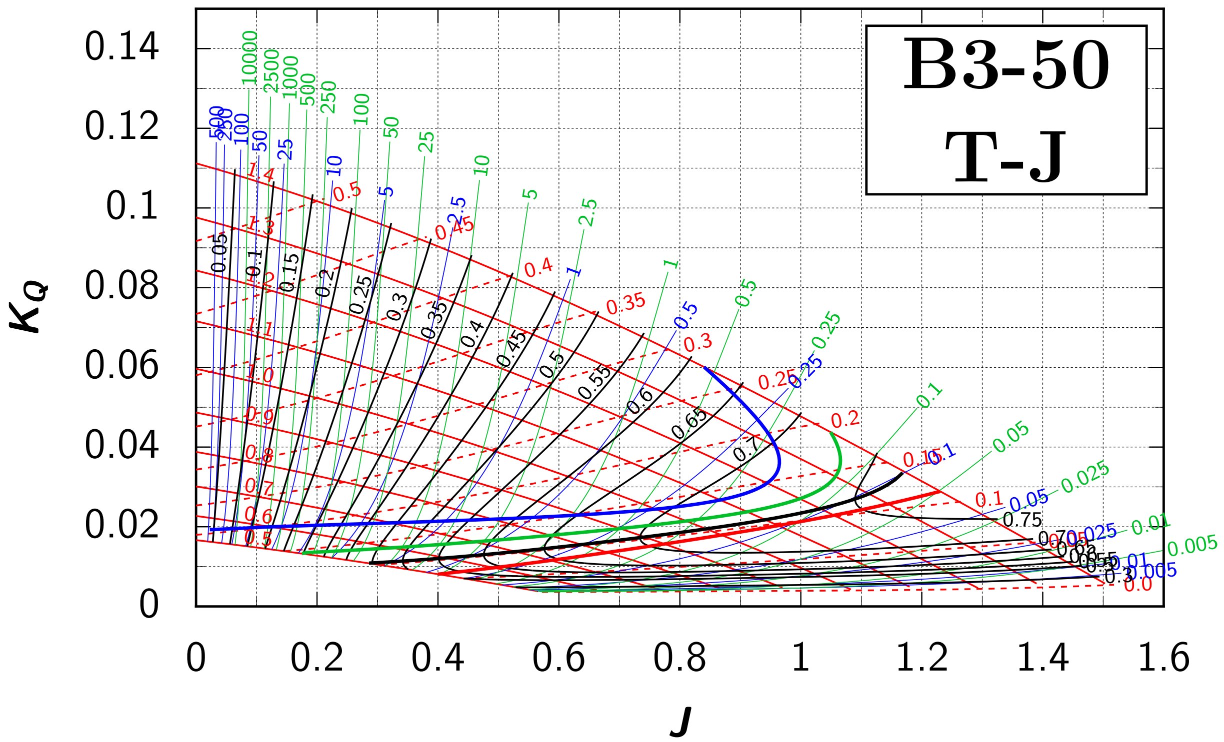

Preprints (www.preprints.org) | NOT PEER-REVIEWED | Posted: 10 December 2019
doi:10.20944/preprints201912.0140.v1

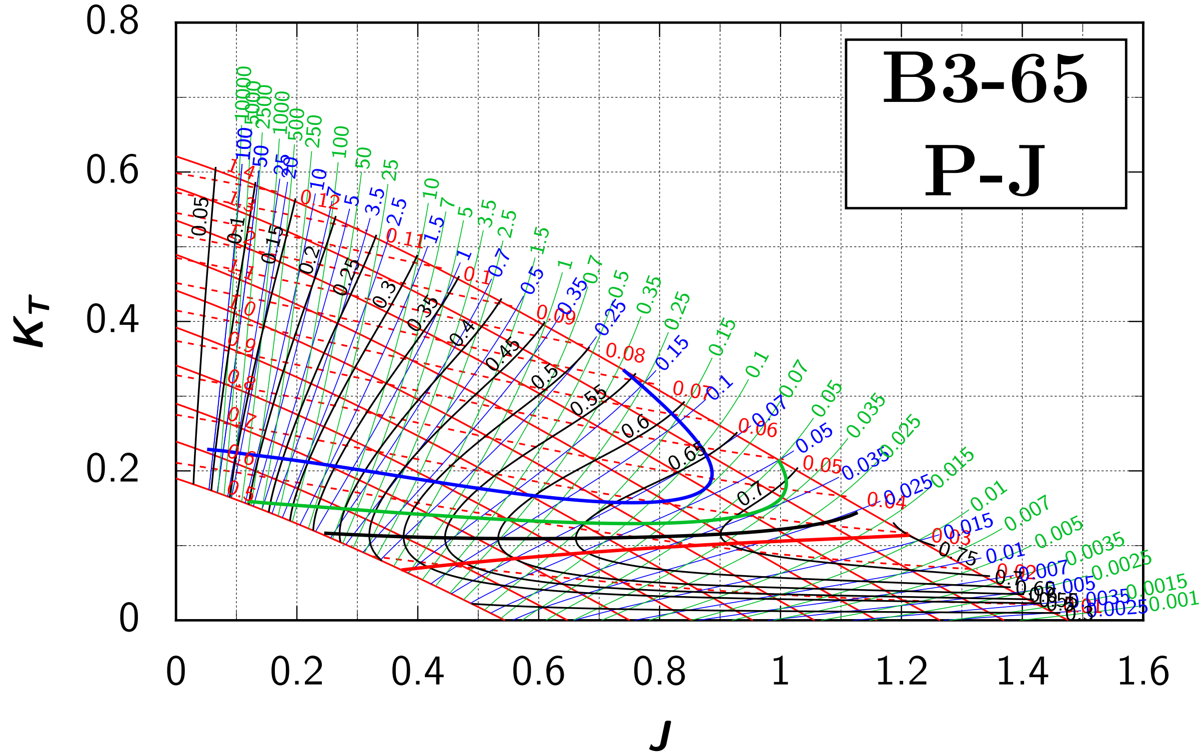

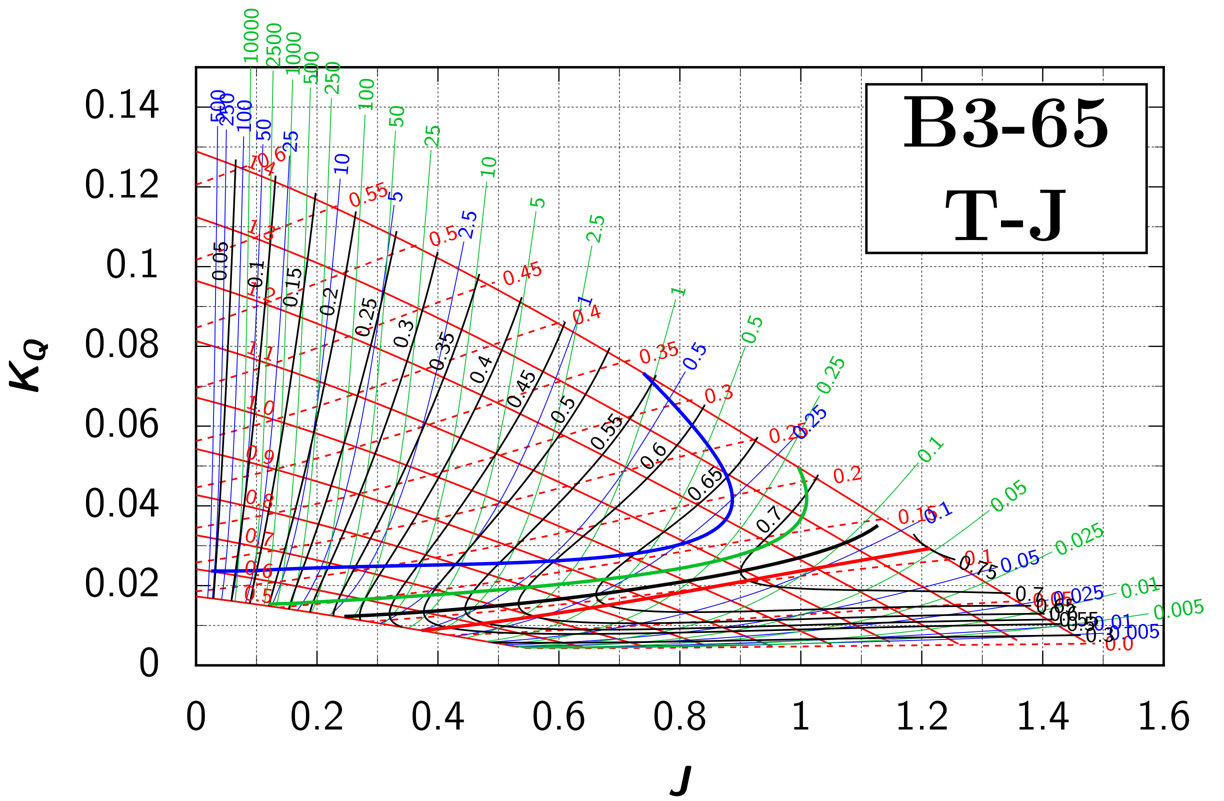

Preprints (www.preprints.org) | NOT PEER-REVIEWED | Posted: 10 December 2019 doi:10.20944/preprints201912.0140.v1

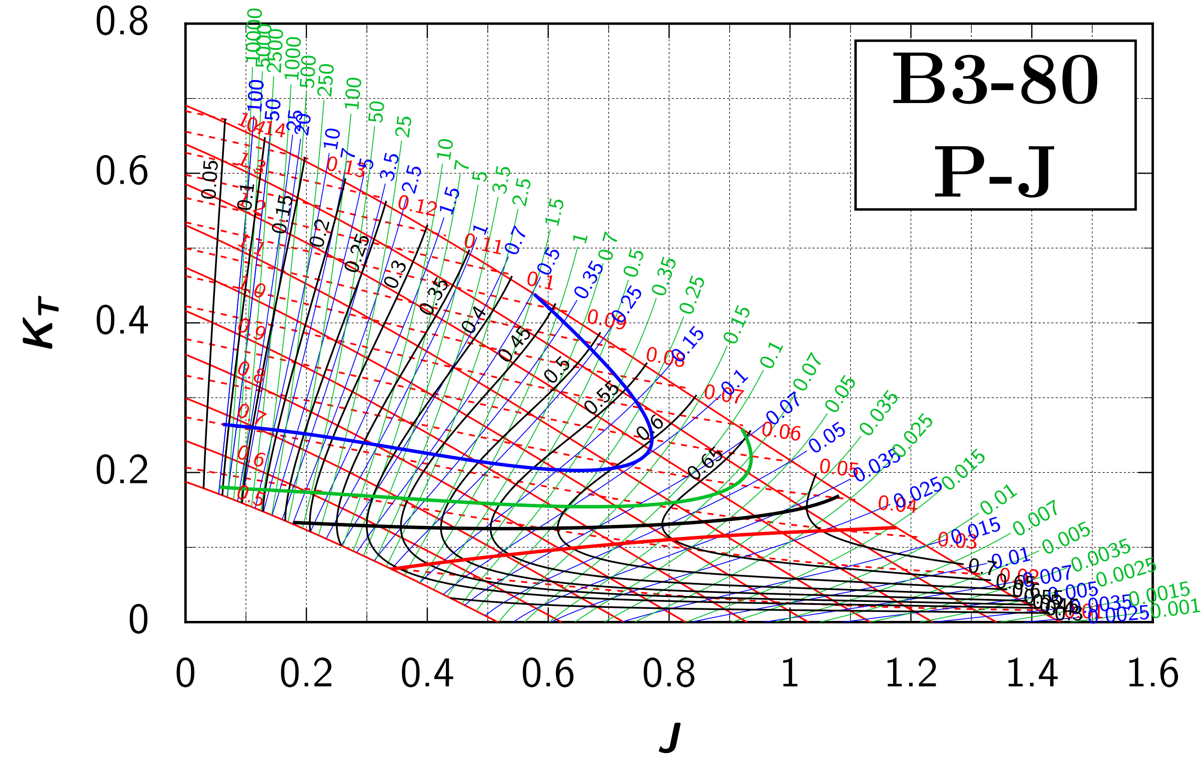

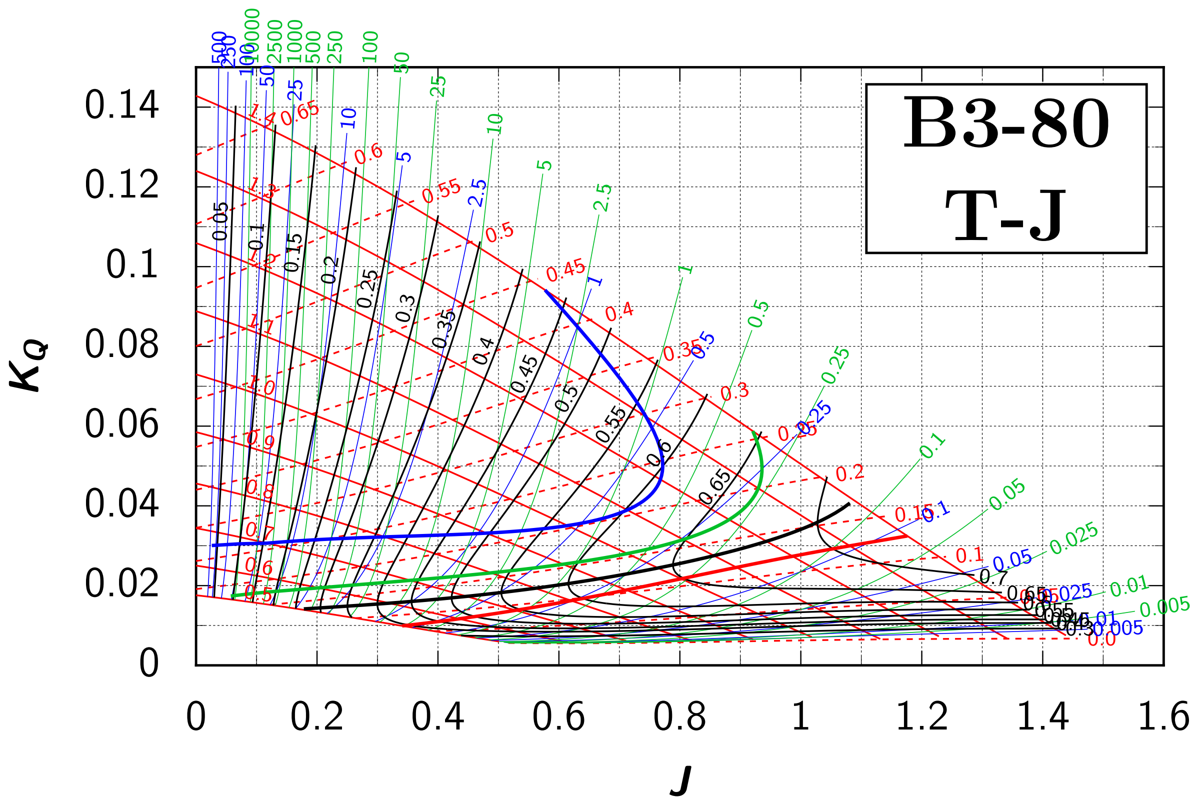

Preprints (www.preprints.org) | NOT PEER-REVIEWED | Posted: 10 December 2019 doi:10.20944/preprints201912.0140.v1

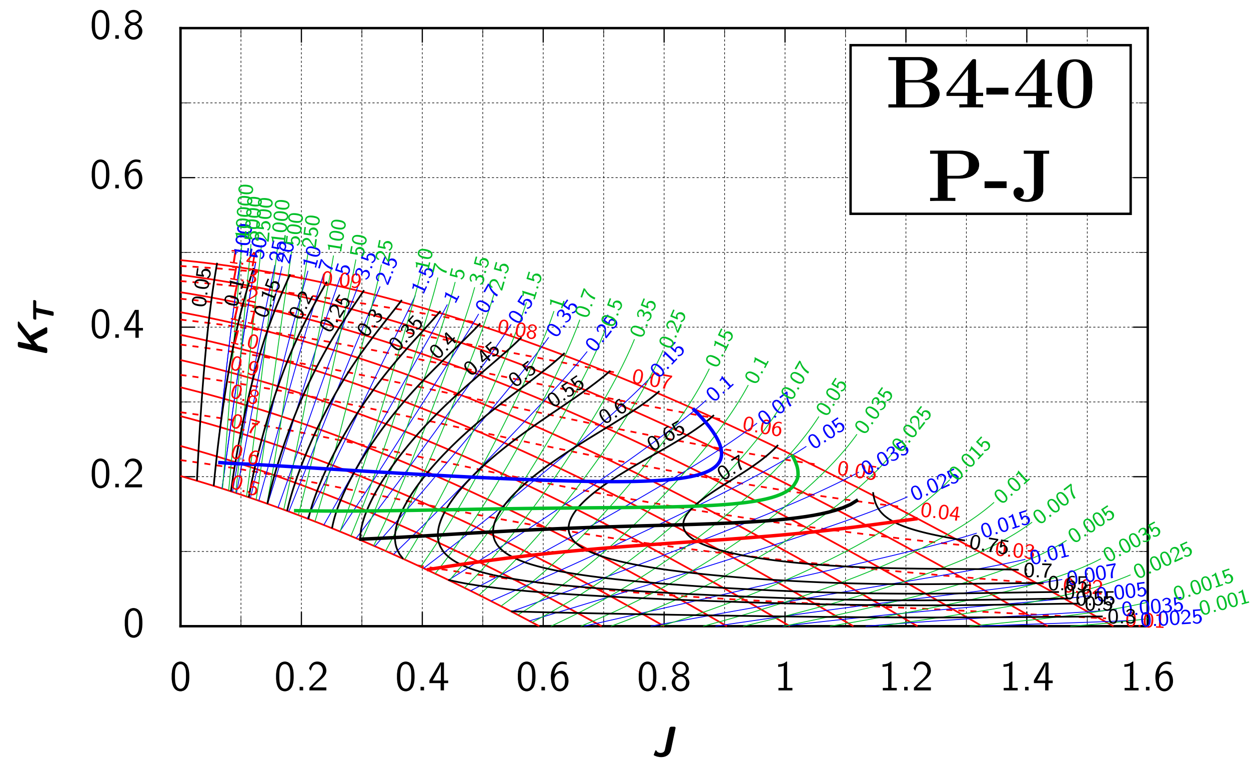

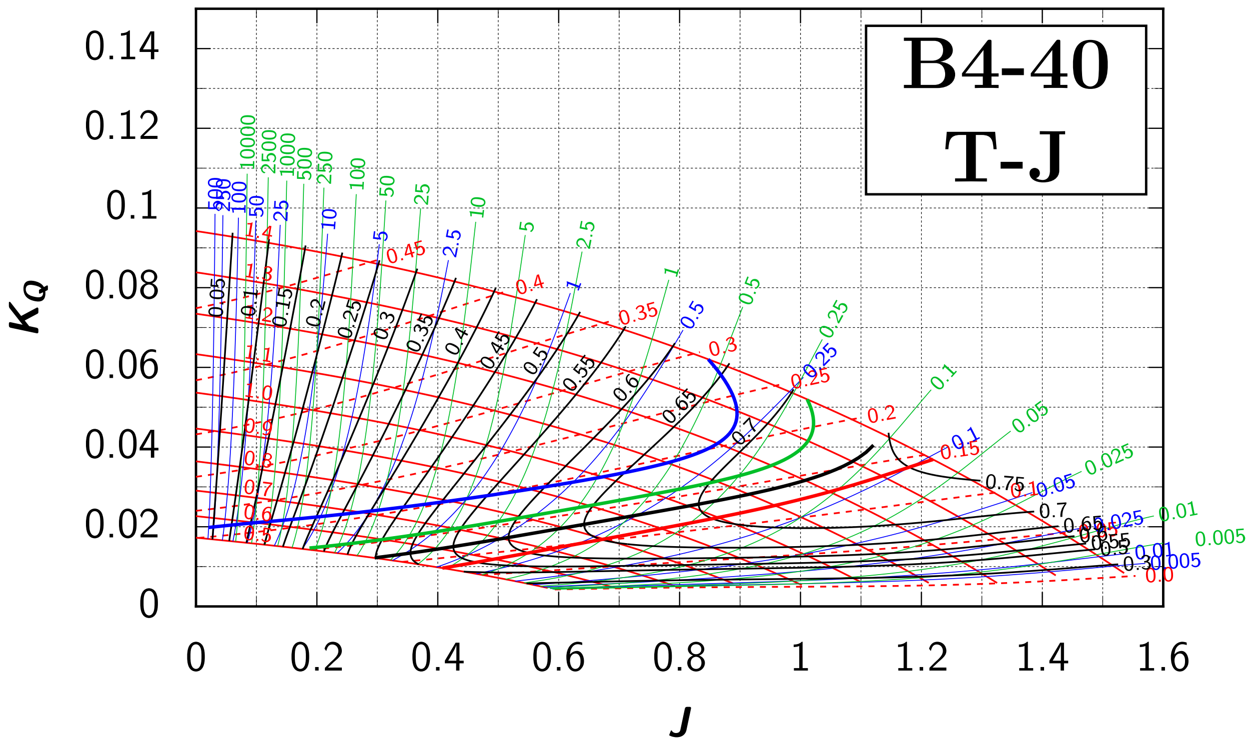

Preprints (www.preprints.org) | NOT PEER-REVIEWED | Posted: 10 December 2019 doi:10.20944/preprints201912.0140.v1

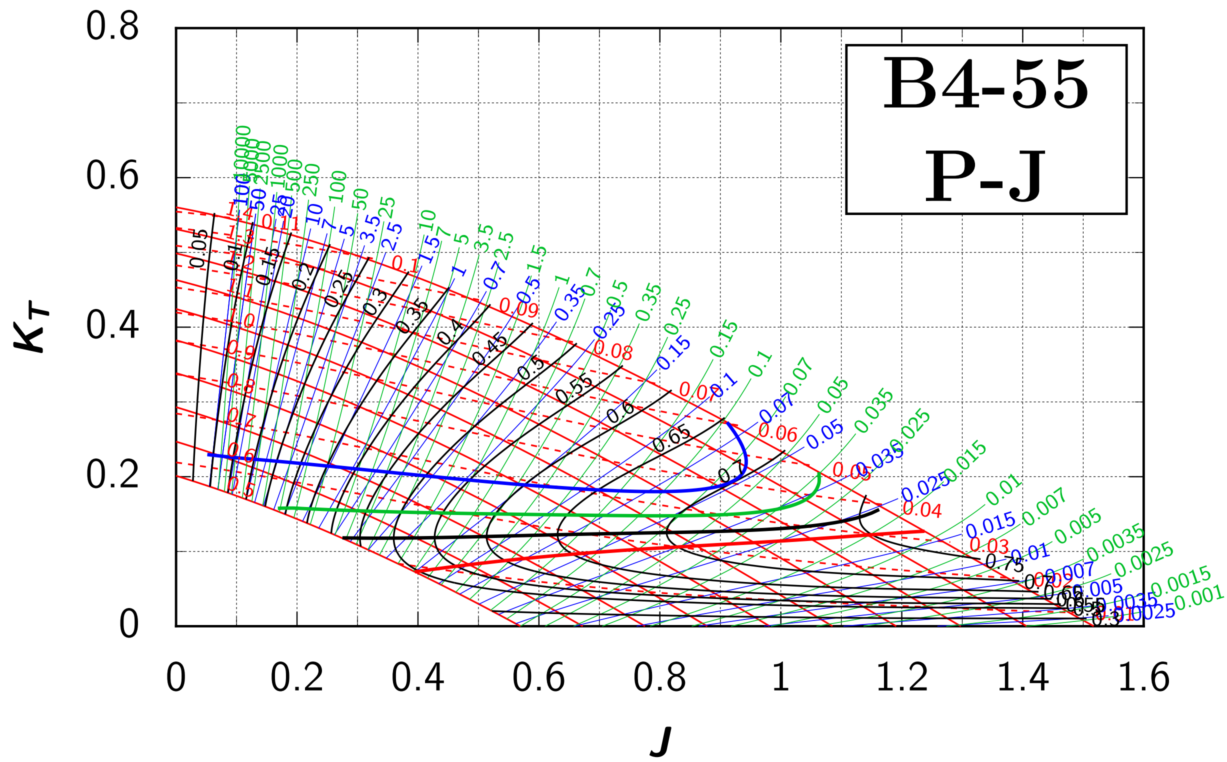

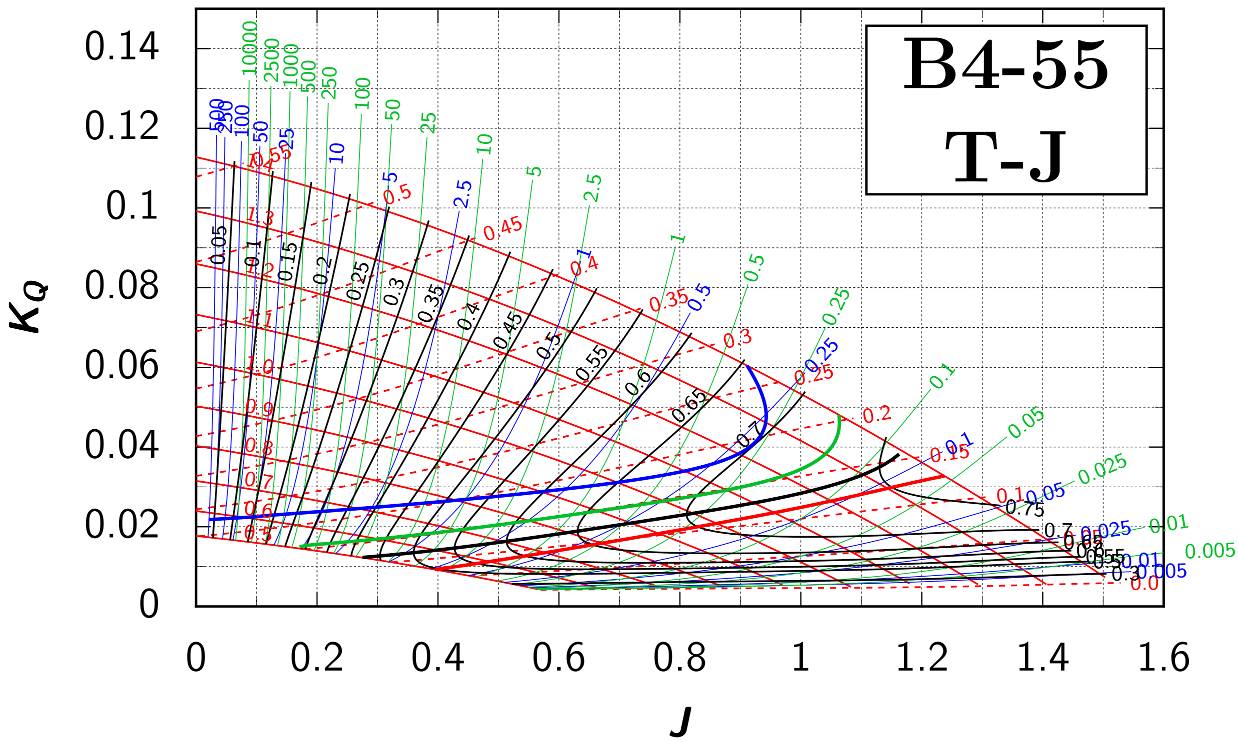

Preprints (www.preprints.org) | NOT PEER-REVIEWED | Posted: 10 December 2019 doi:10.20944/preprints201912.0140.v1

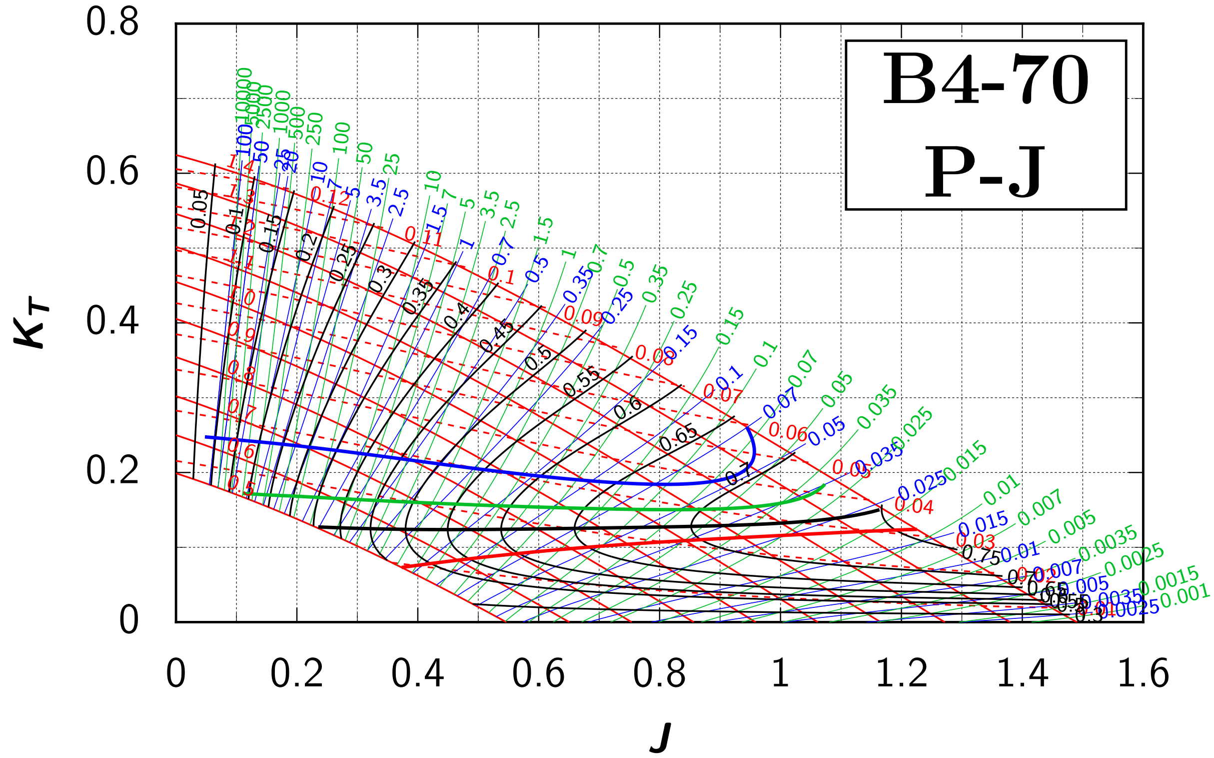

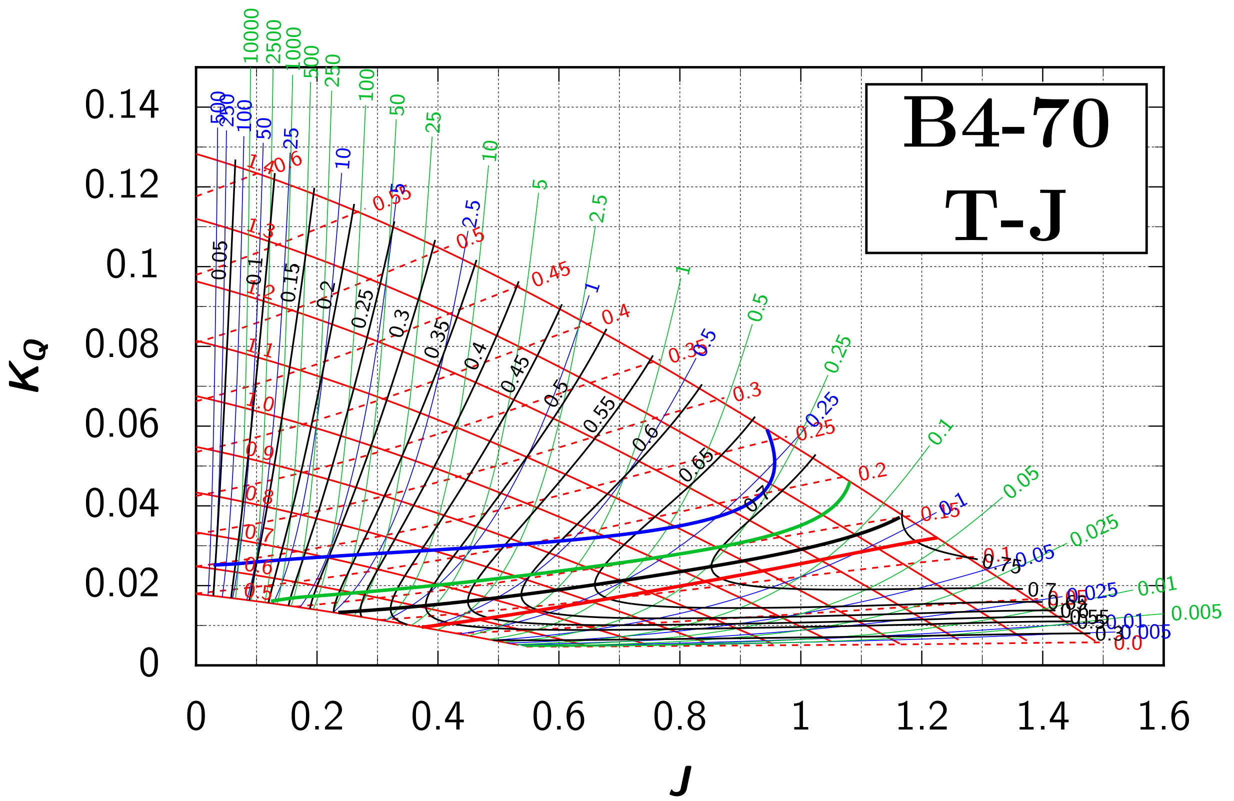

Preprints (www.preprints.org) | NOT PEER-REVIEWED | Posted: 10 December 2019 doi:10.20944/preprints201912.0140.v1

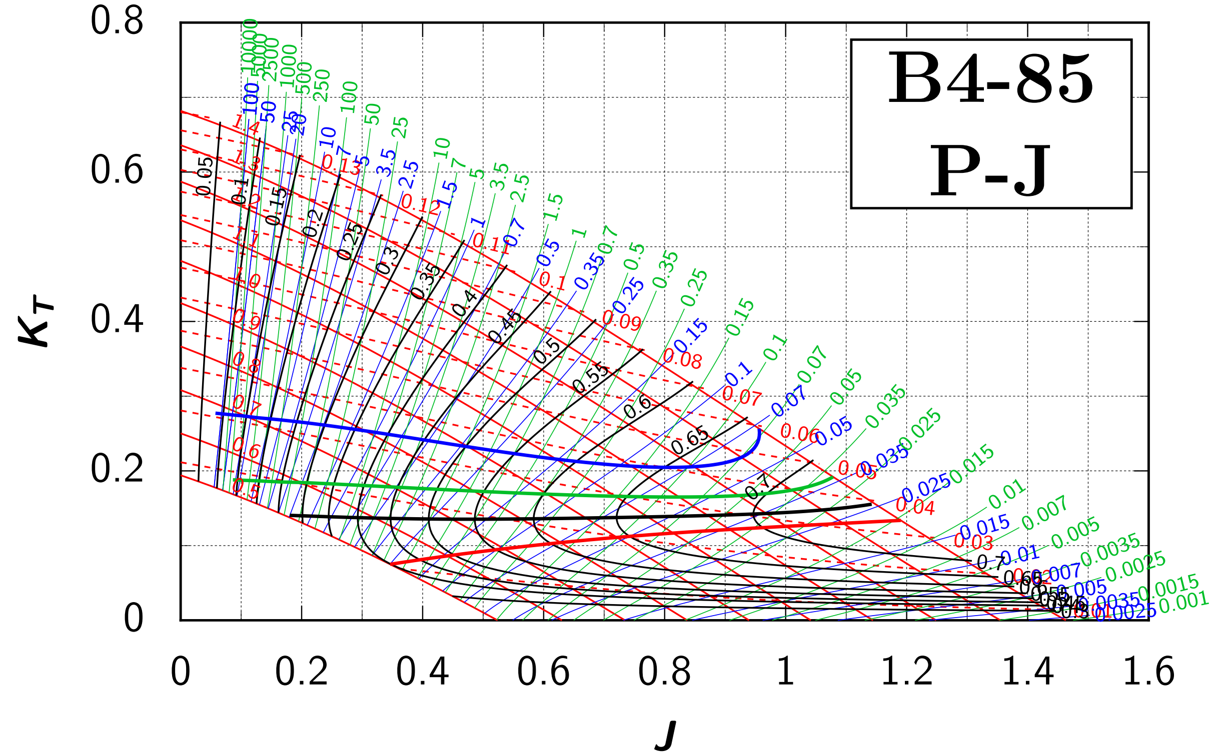

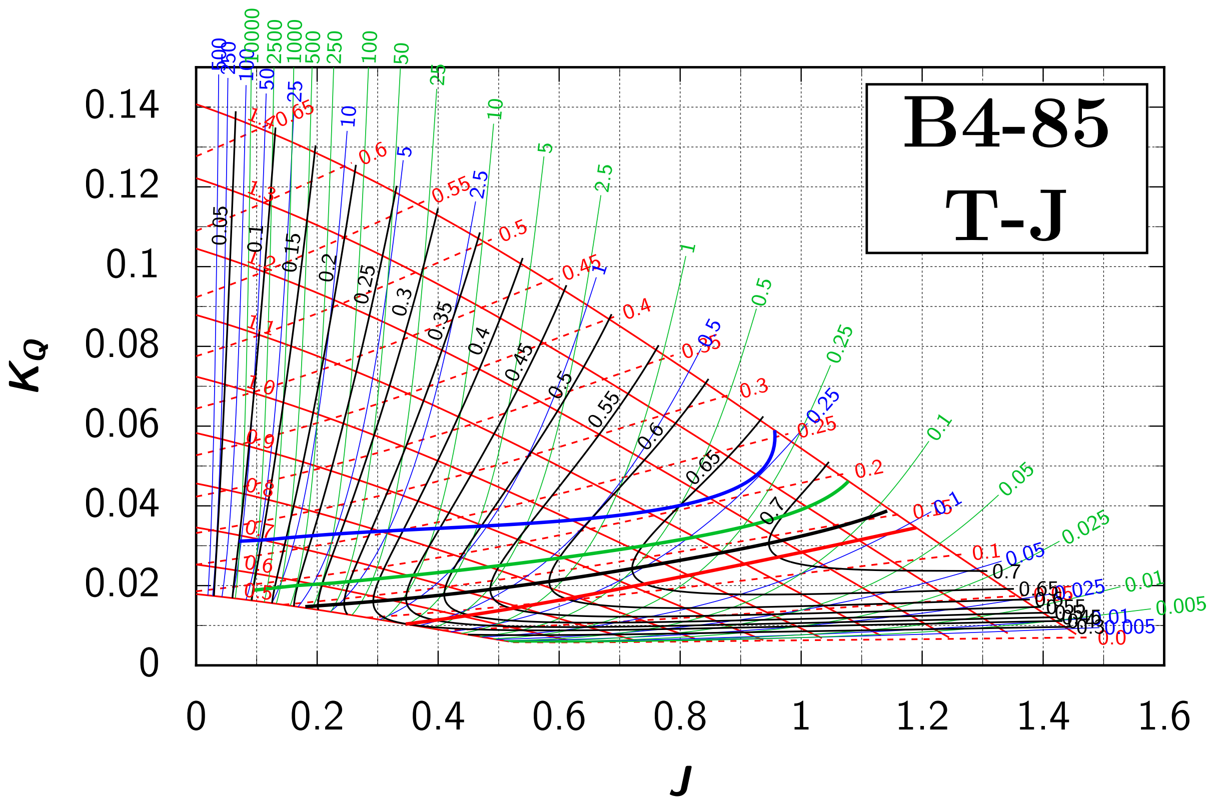

Preprints (www.preprints.org) | NOT PEER-REVIEWED | Posted: 10 December 2019
doi:10.20944/preprints201912.0140.v1

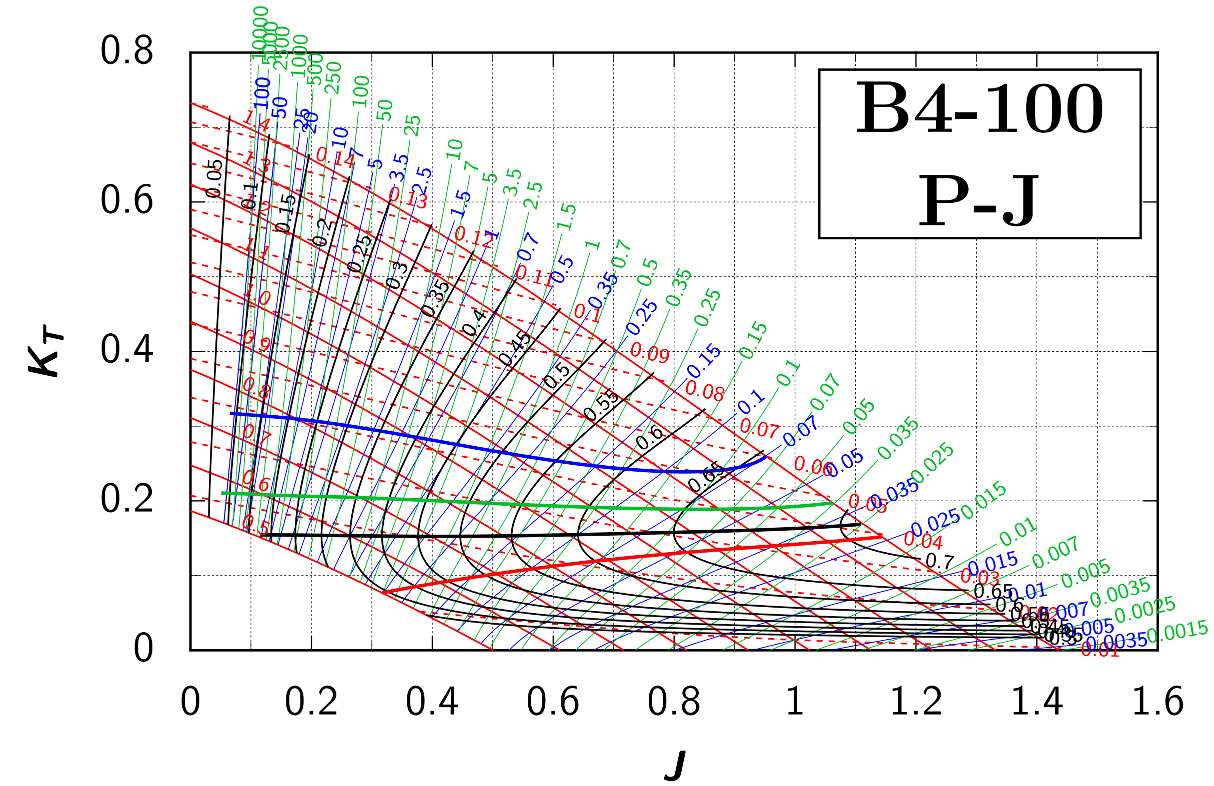

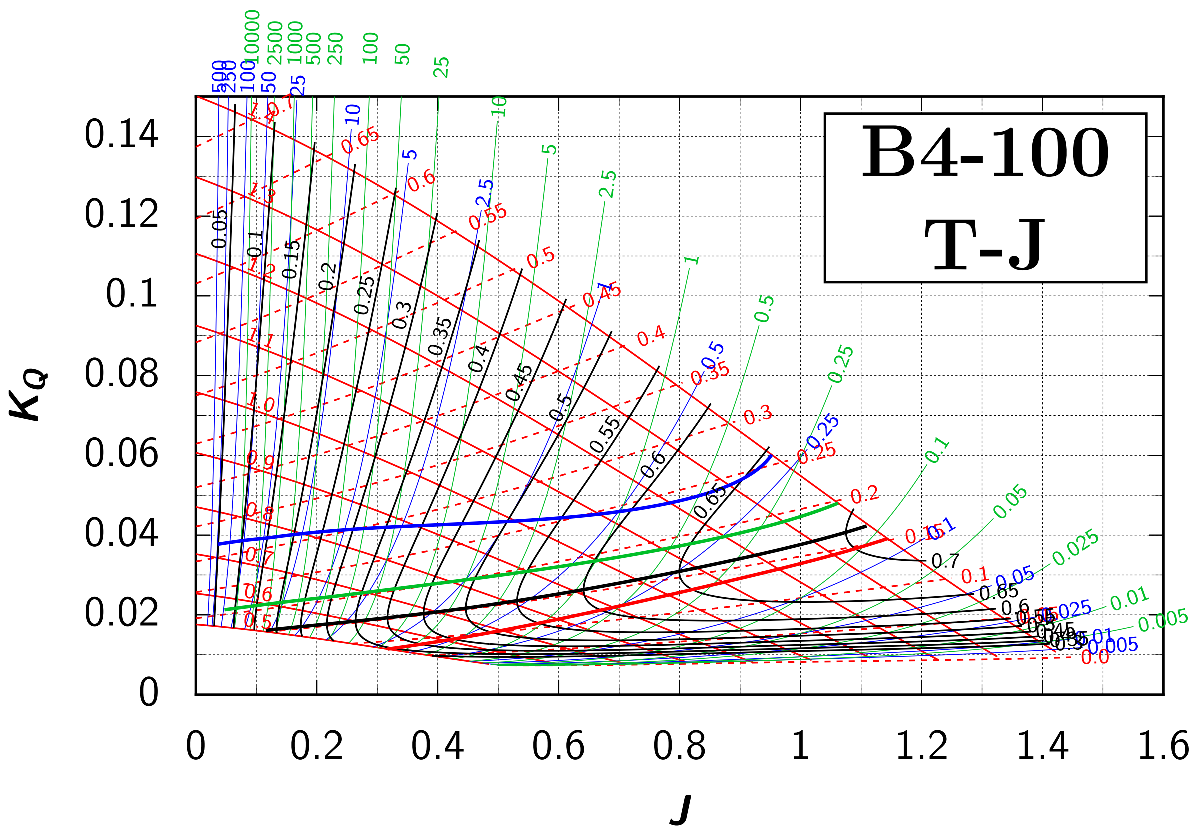

Preprints (www.preprints.org) | NOT PEER-REVIEWED | Posted: 10 December 2019 doi:10.20944/preprints201912.0140.v1

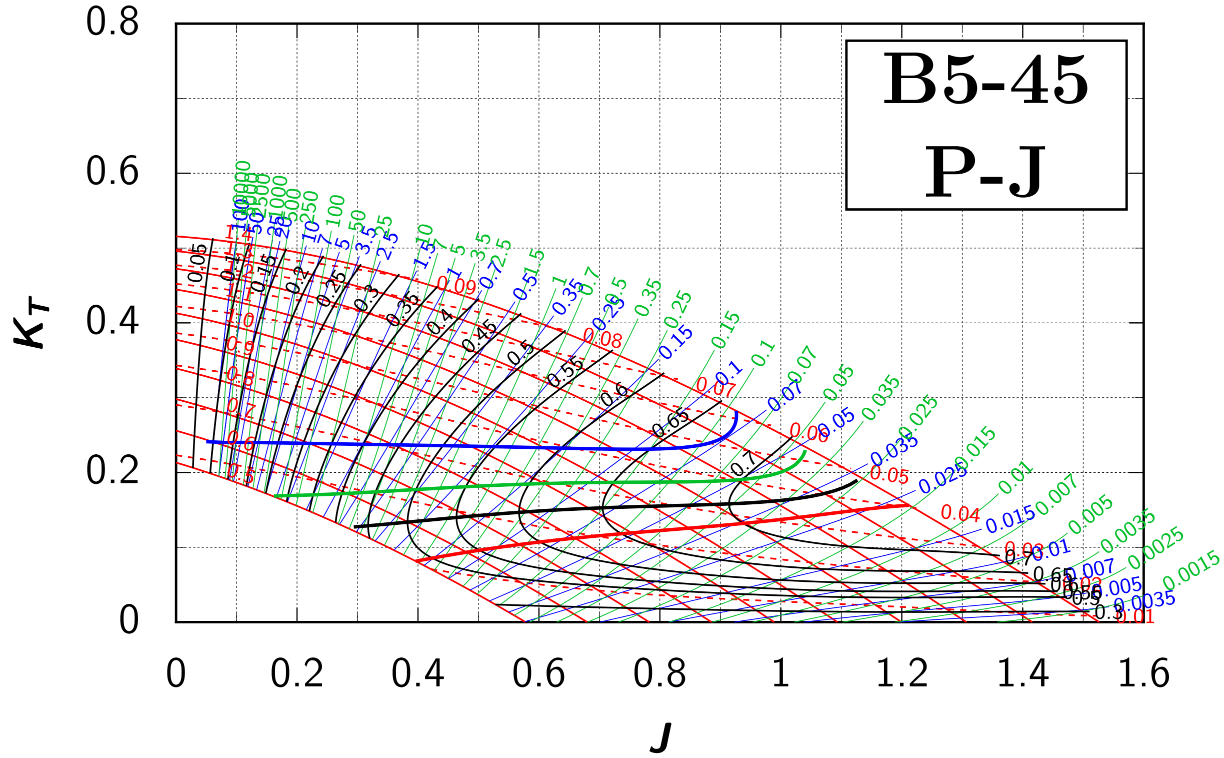

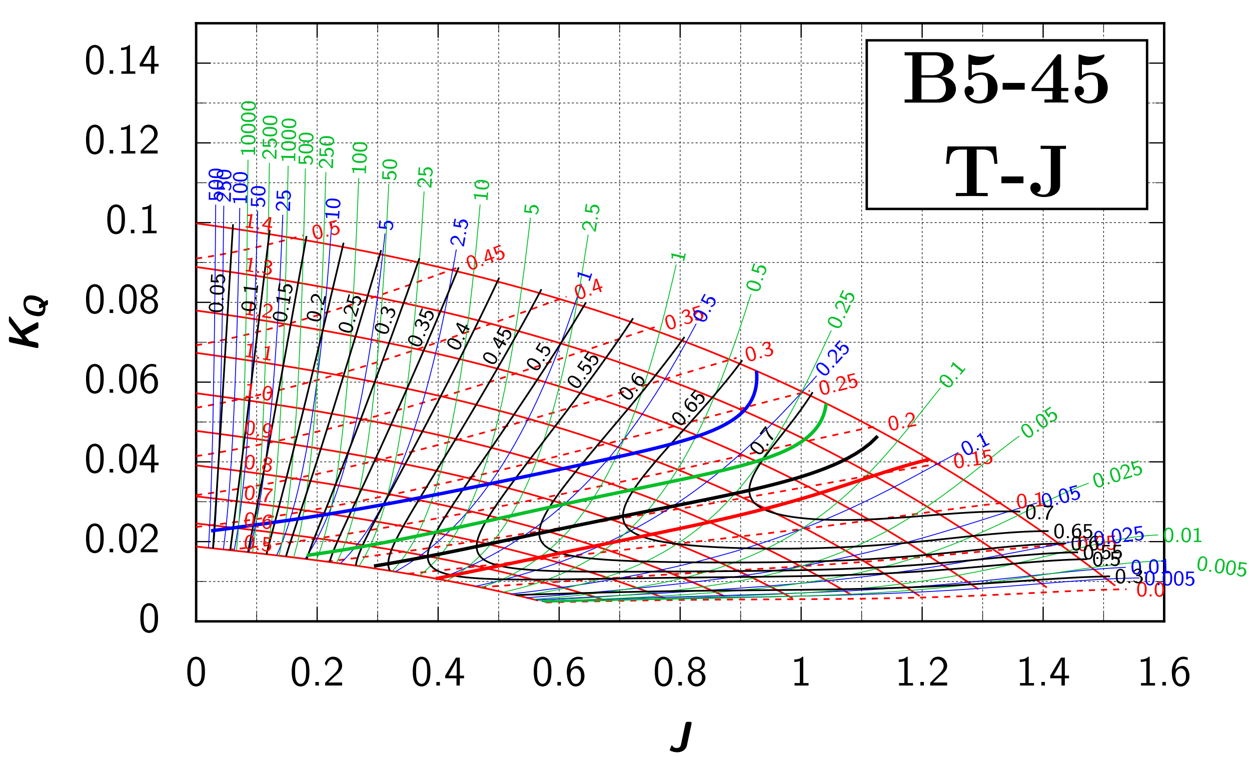

Preprints (www.preprints.org) | NOT PEER-REVIEWED | Posted: 10 December 2019 doi:10.20944/preprints201912.0140.v1

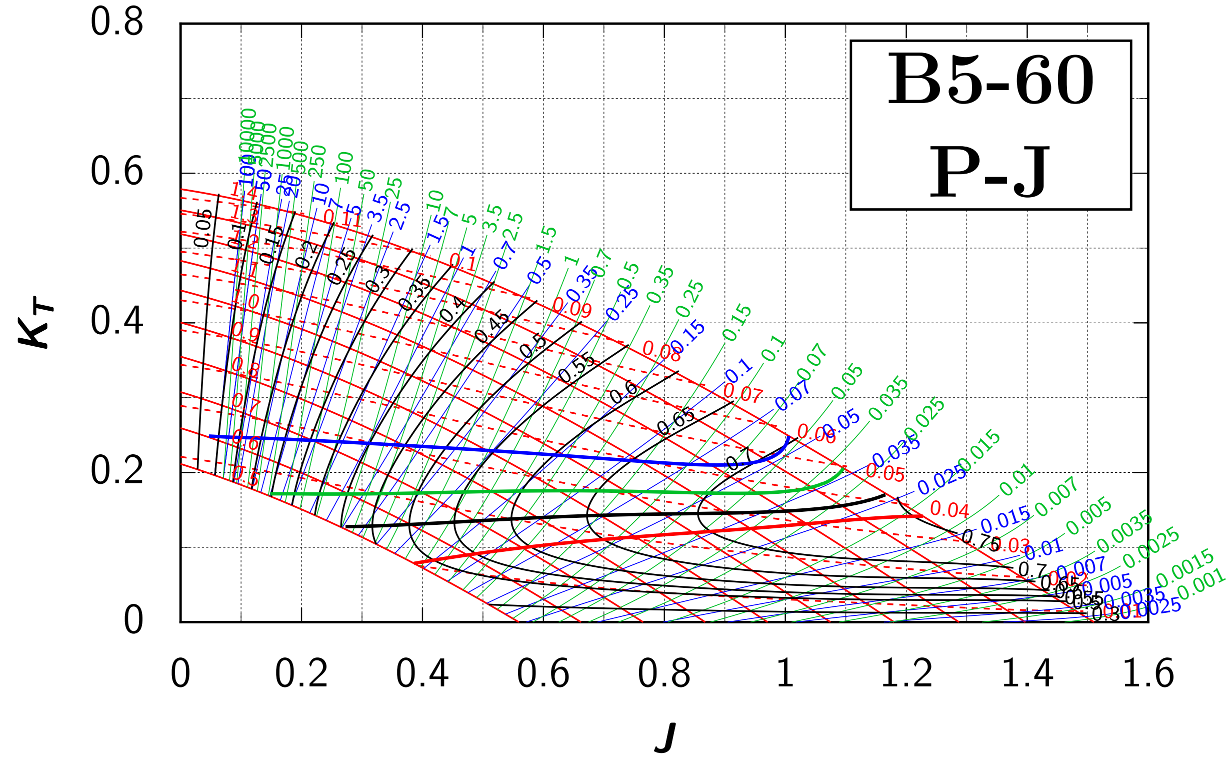

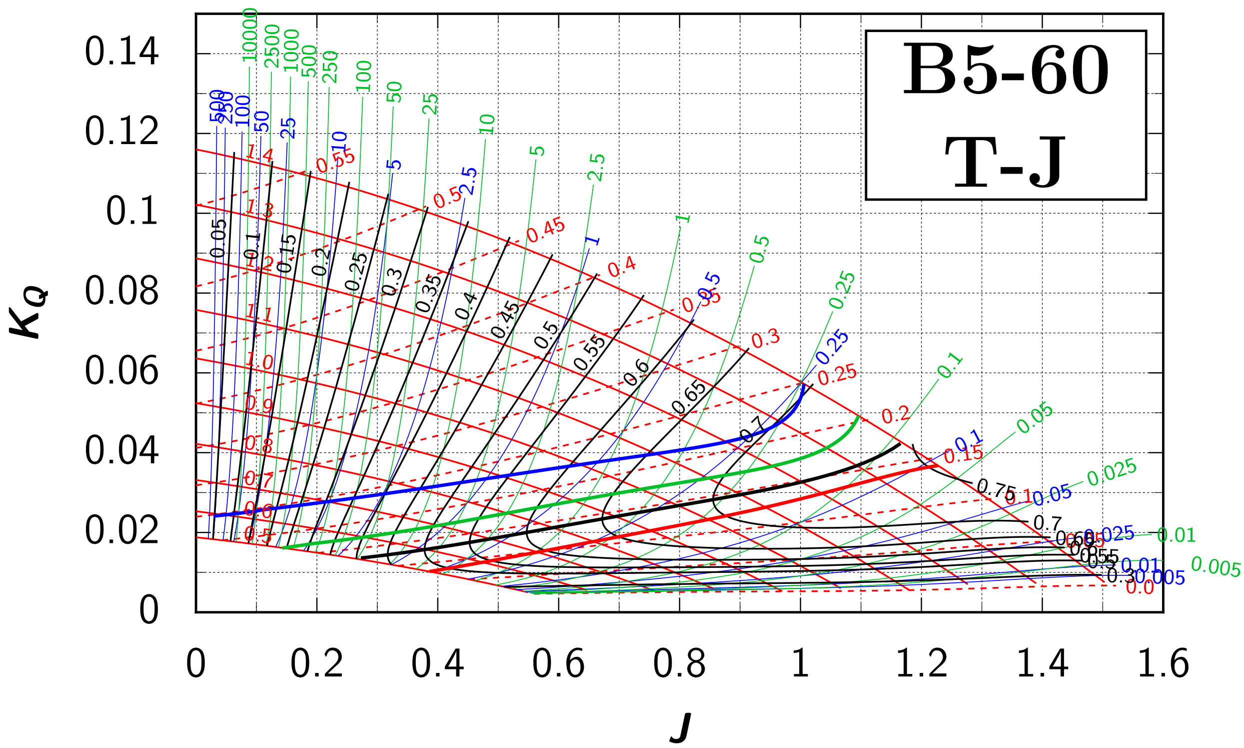

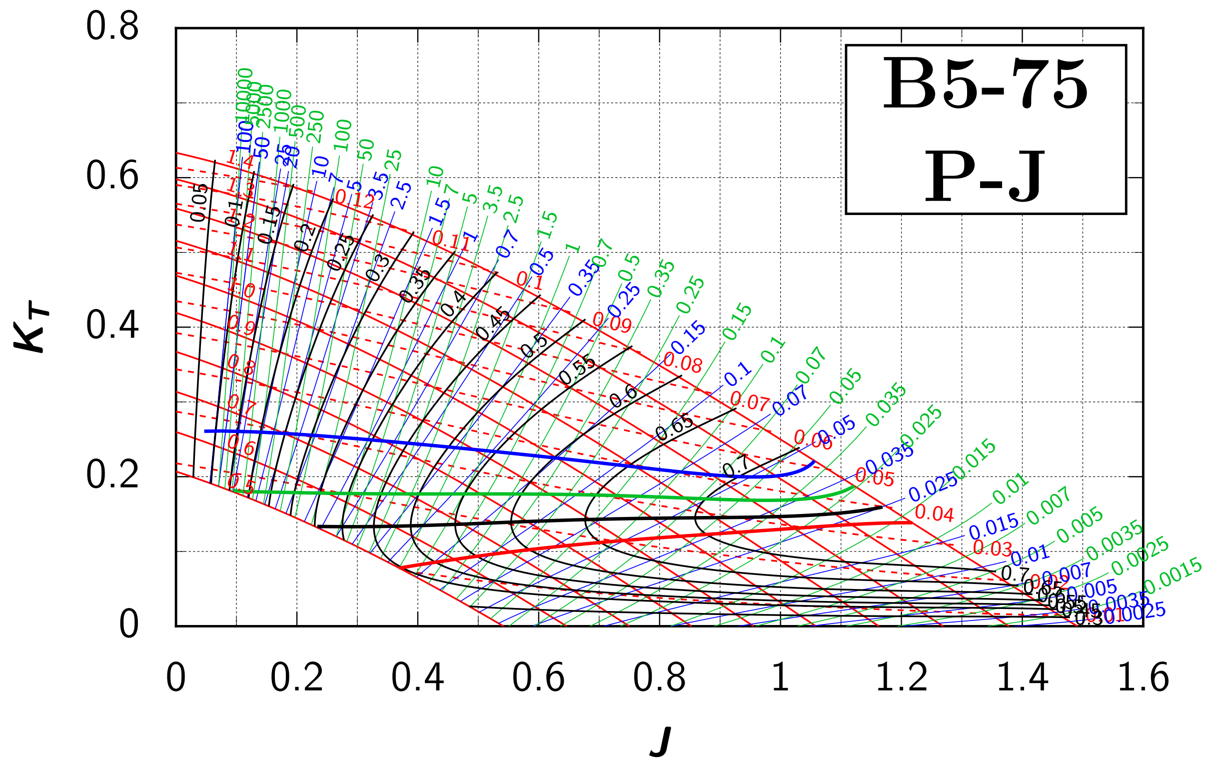
B5-75
P-J
K_T
J

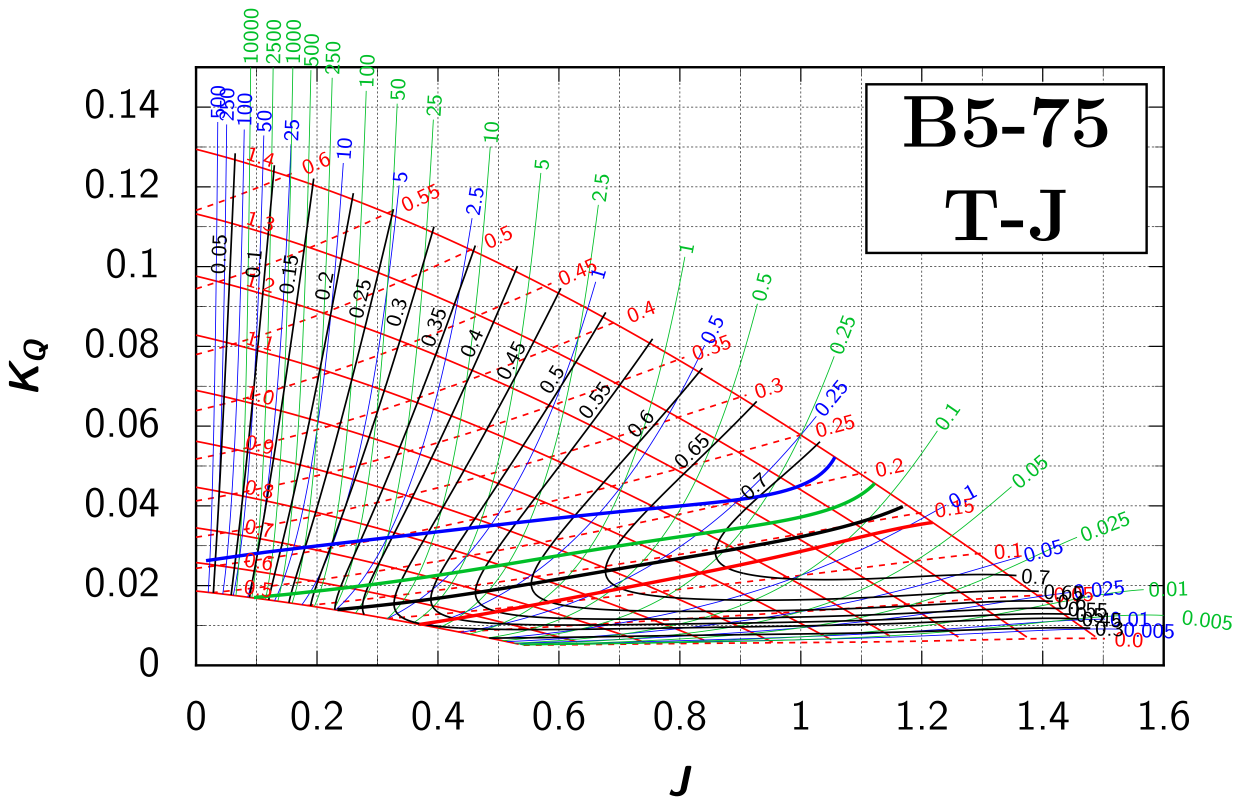
B5-75
T-J
K_Q
J

Preprints (www.preprints.org) | NOT PEER-REVIEWED | Posted: 10 December 2019 doi:10.20944/preprints201912.0140.v1

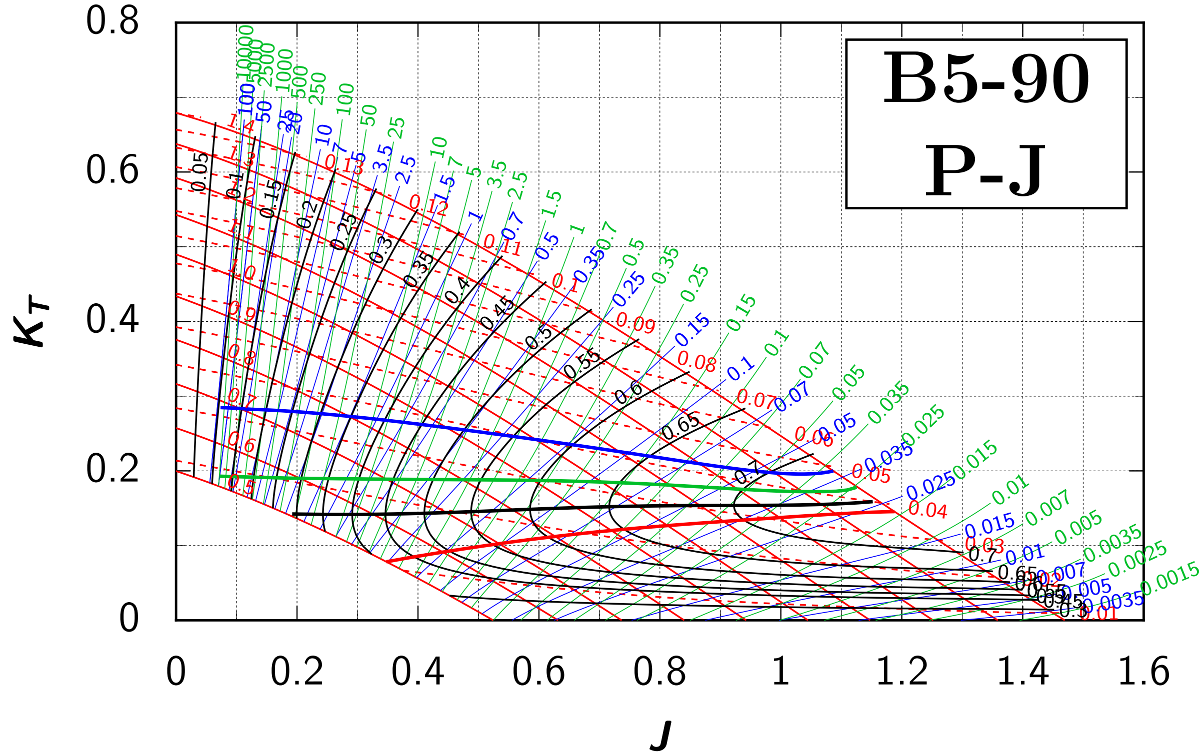

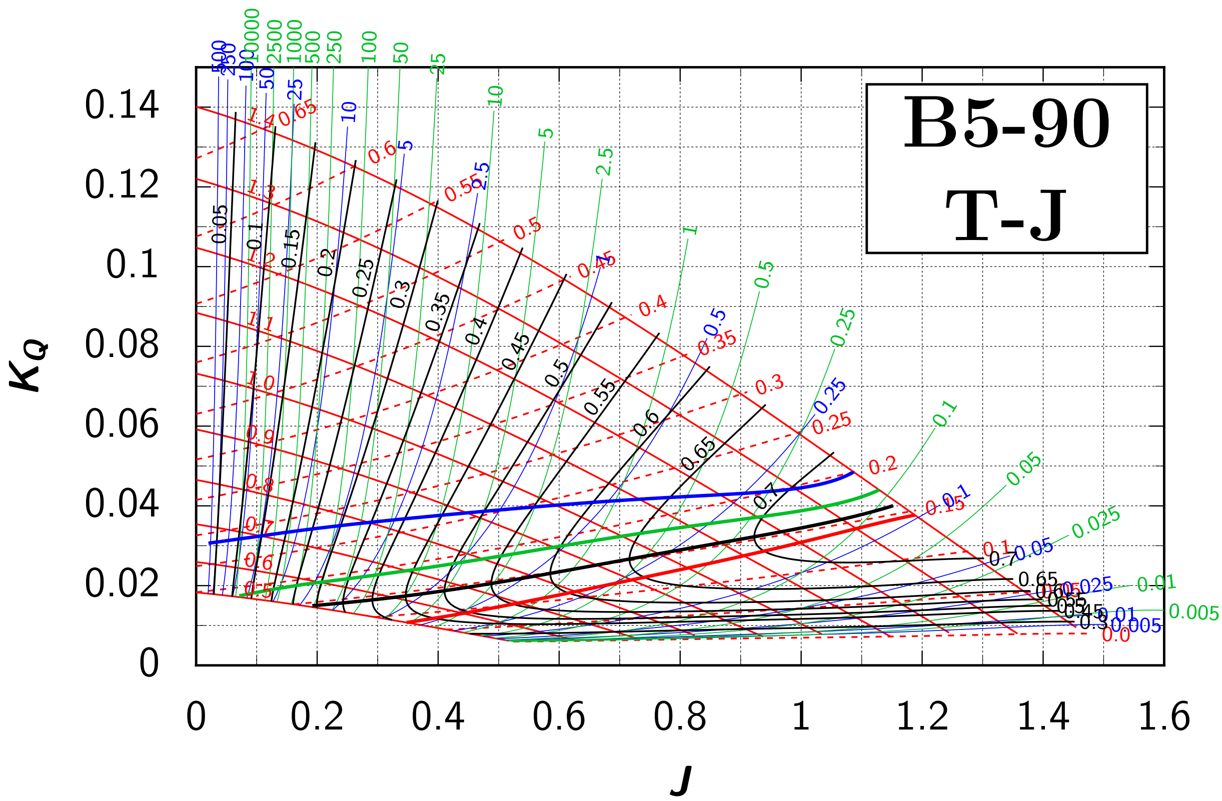

Preprints (www.preprints.org) | NOT PEER-REVIEWED | Posted: 10 December 2019 doi:10.20944/preprints201912.0140.v1

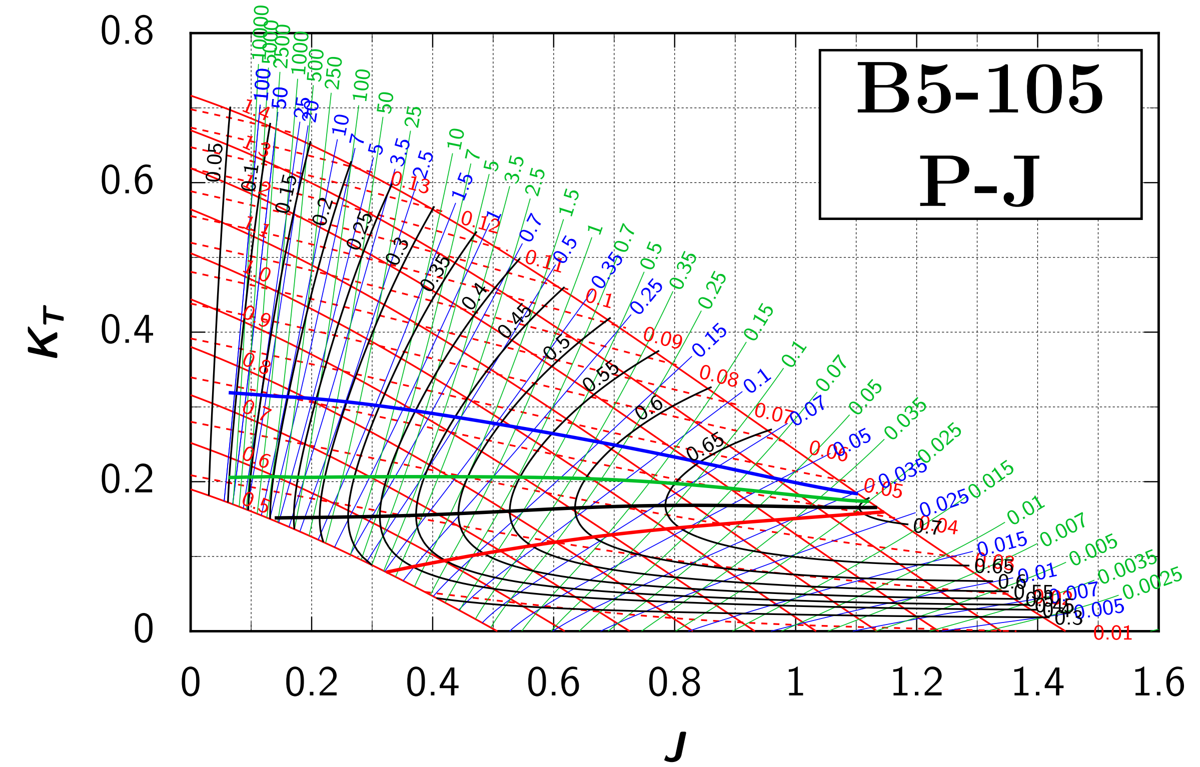

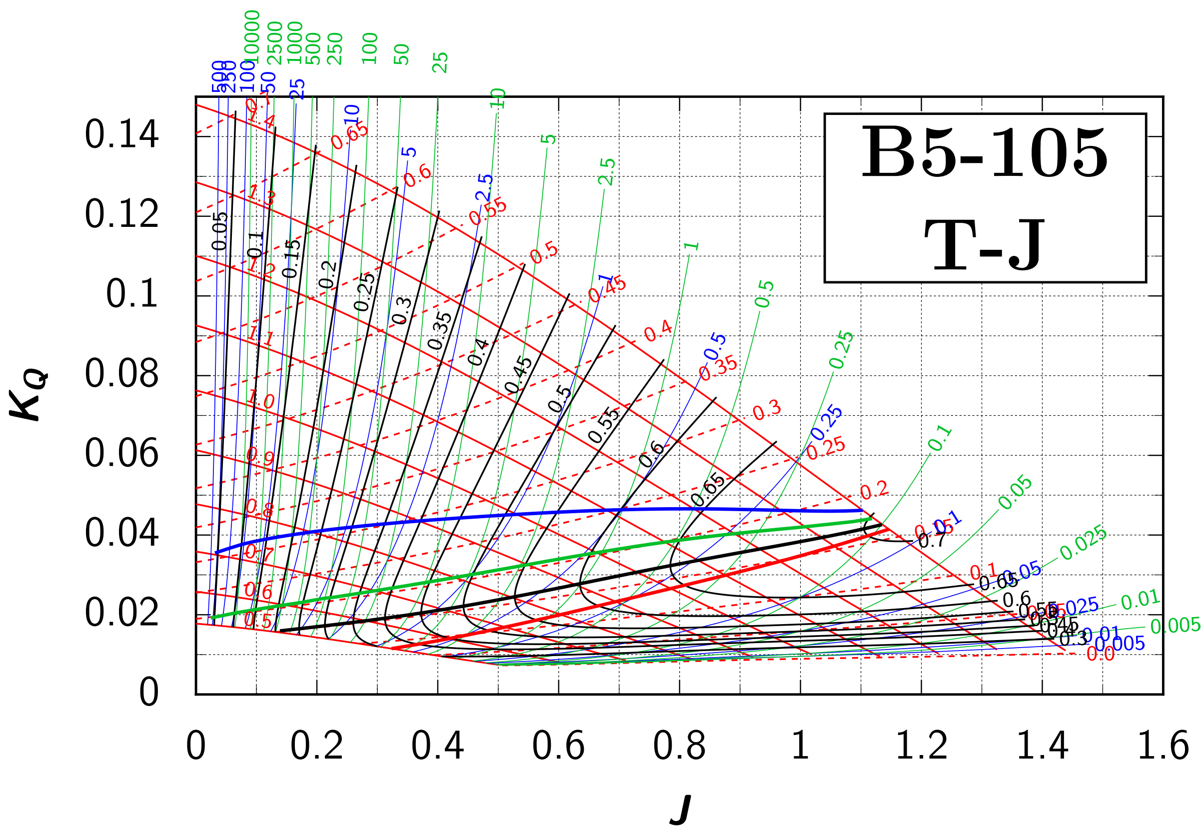

Preprints (www.preprints.org) | NOT PEER-REVIEWED | Posted: 10 December 2019 doi:10.20944/preprints201912.0140.v1

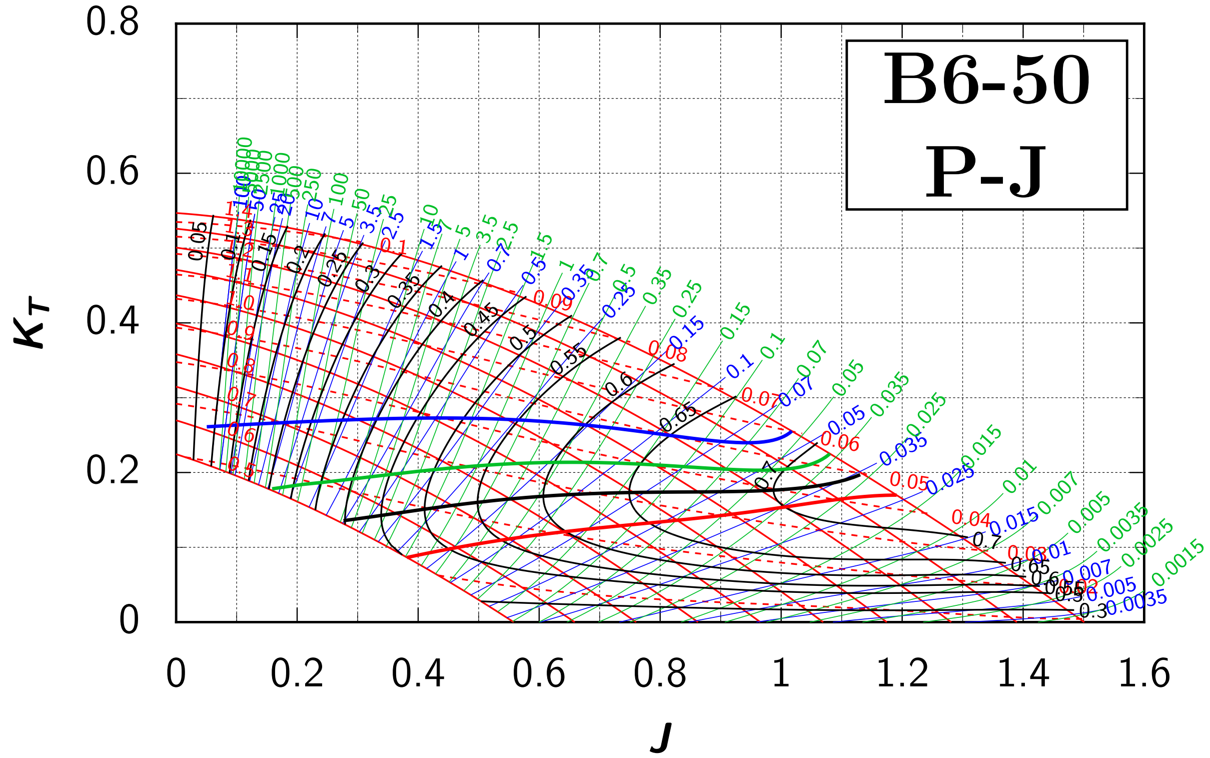

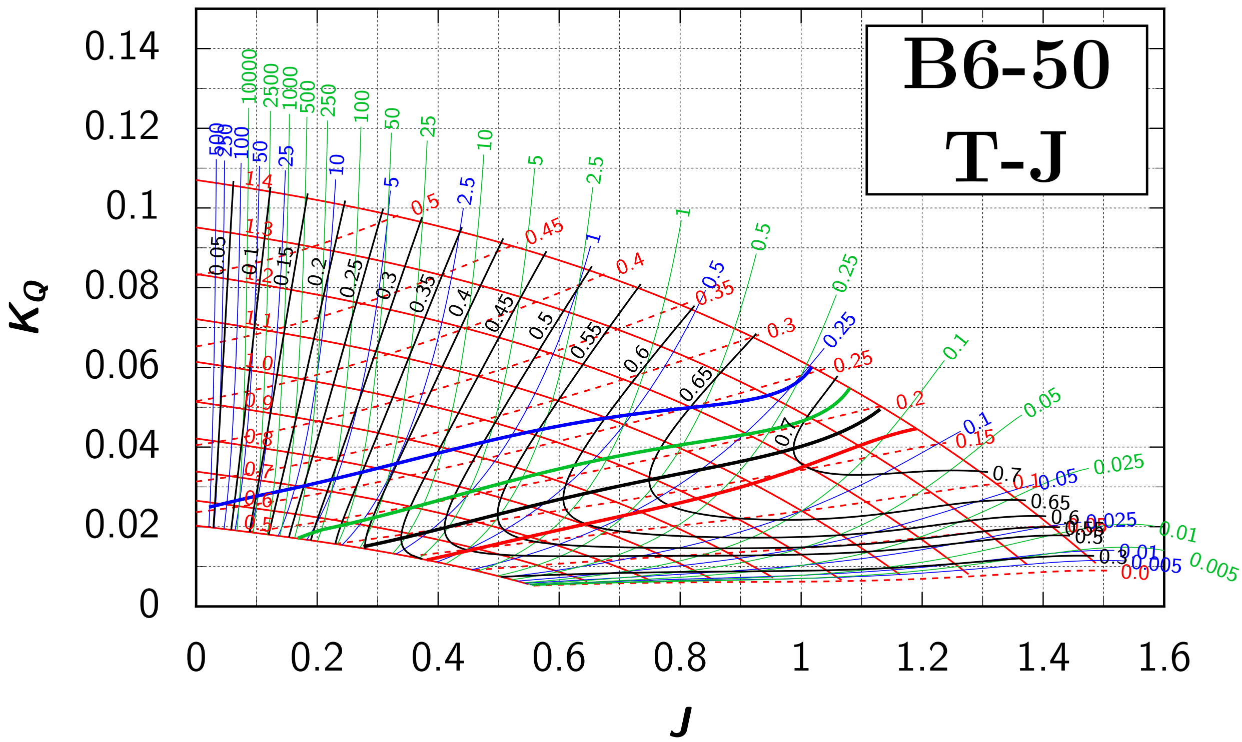

Preprints (www.preprints.org) | NOT PEER-REVIEWED | Posted: 10 December 2019 doi:10.20944/preprints201912.0140.v1

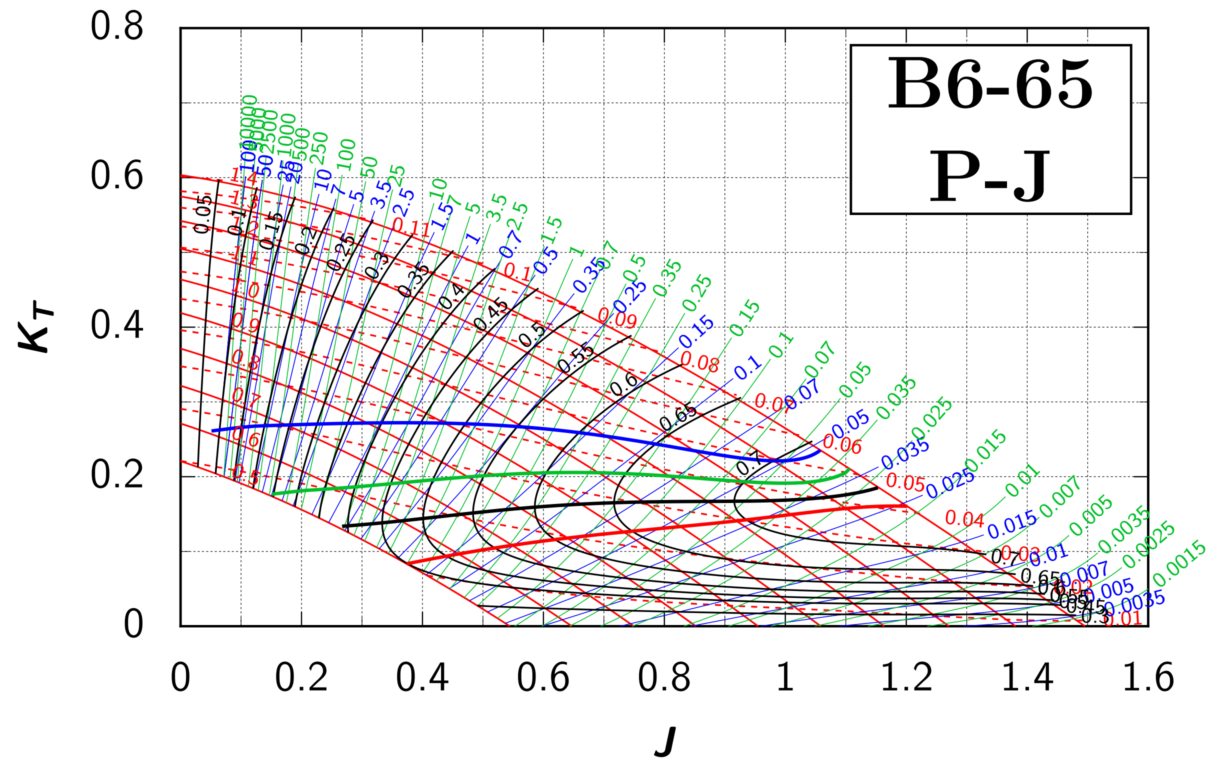

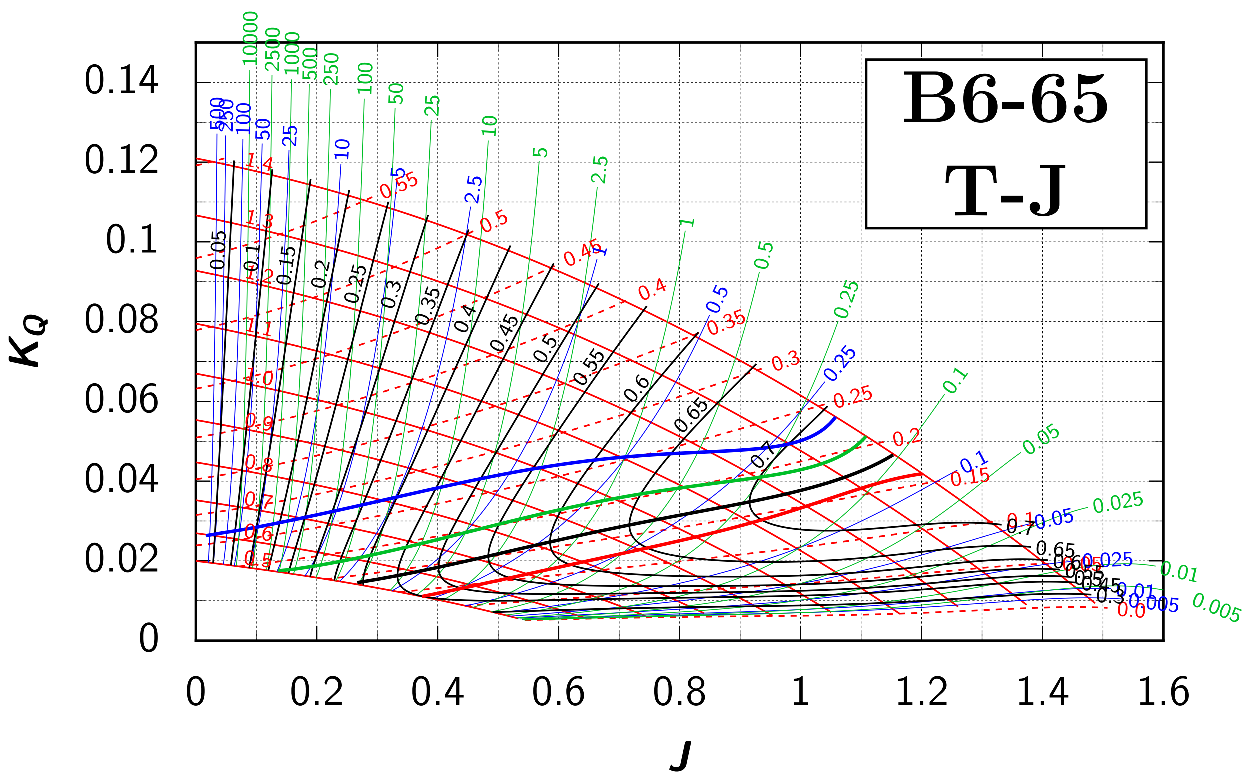

Preprints (www.preprints.org) | NOT PEER-REVIEWED | Posted: 10 December 2019 doi:10.20944/preprints201912.0140.v1

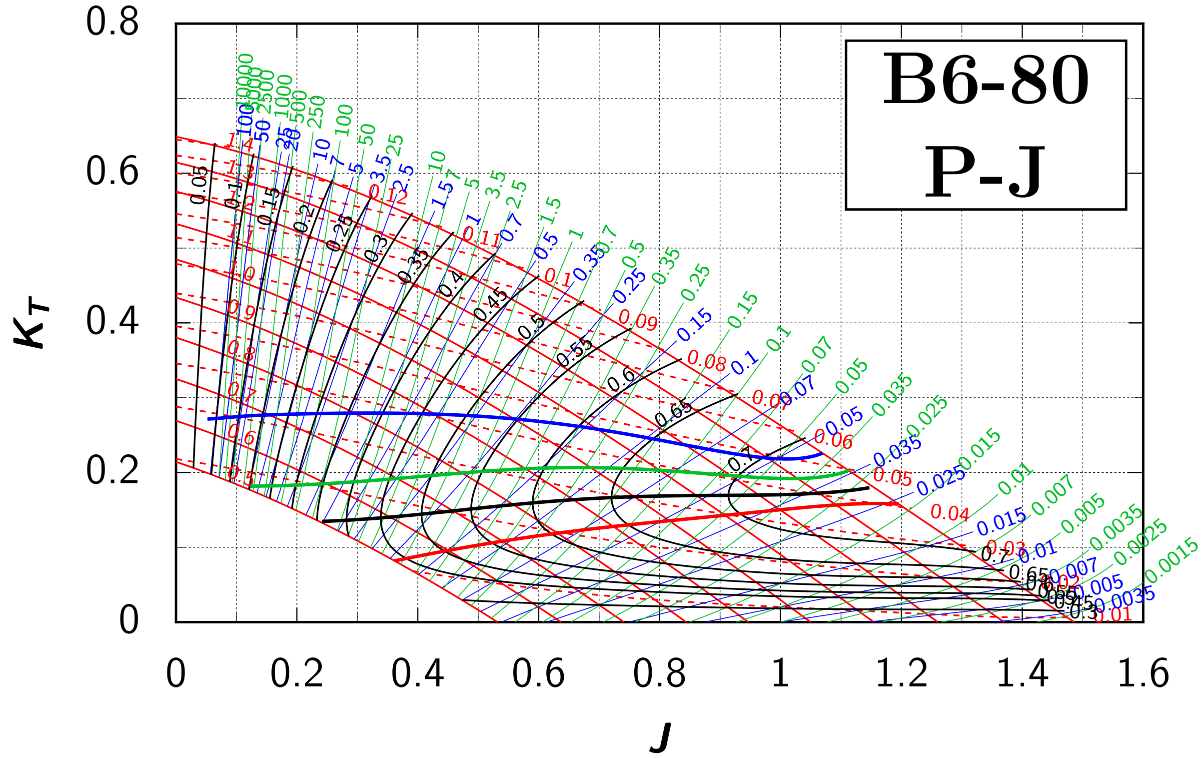

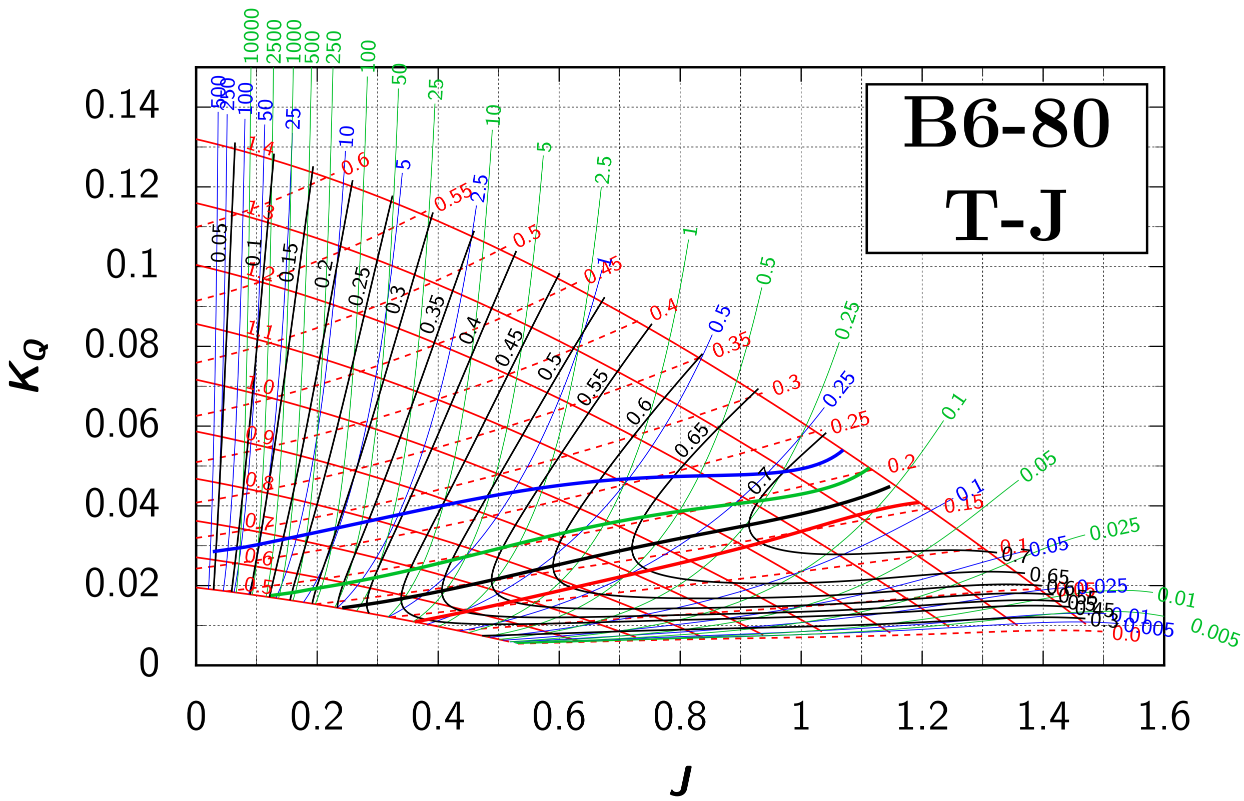

Preprints (www.preprints.org) | NOT PEER-REVIEWED | Posted: 10 December 2019 doi:10.20944/preprints201912.0140.v1

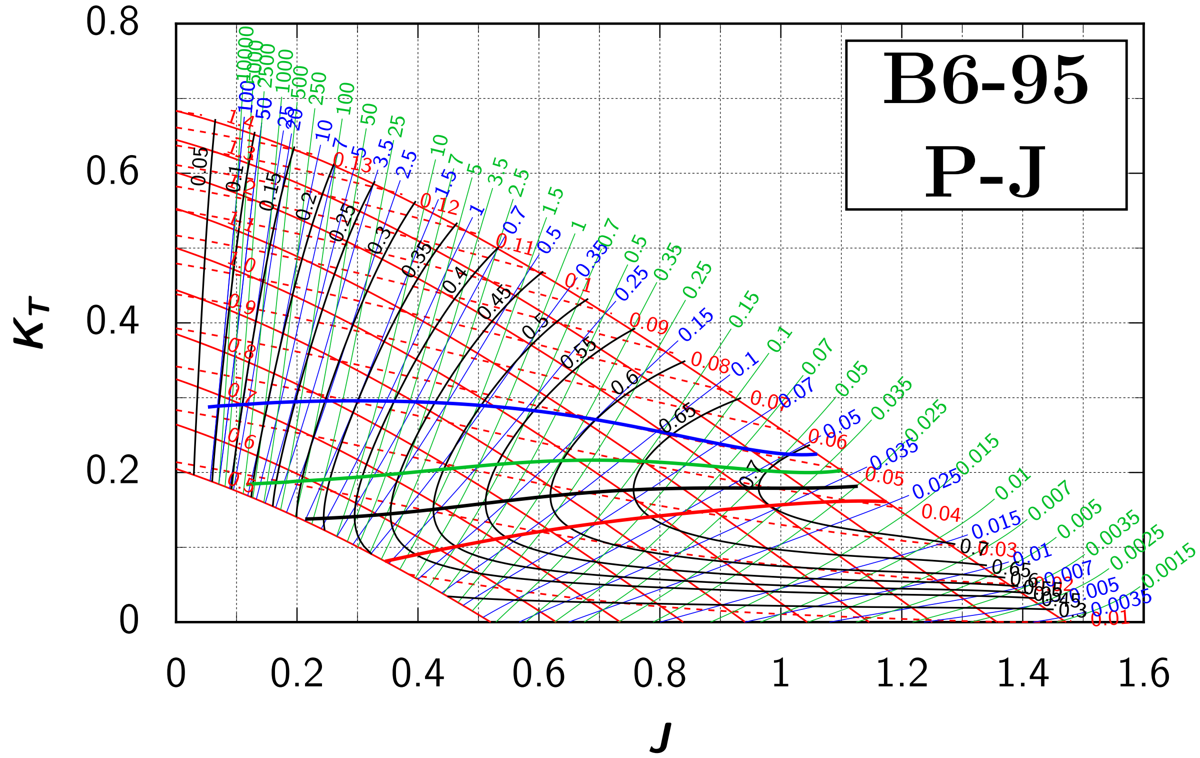

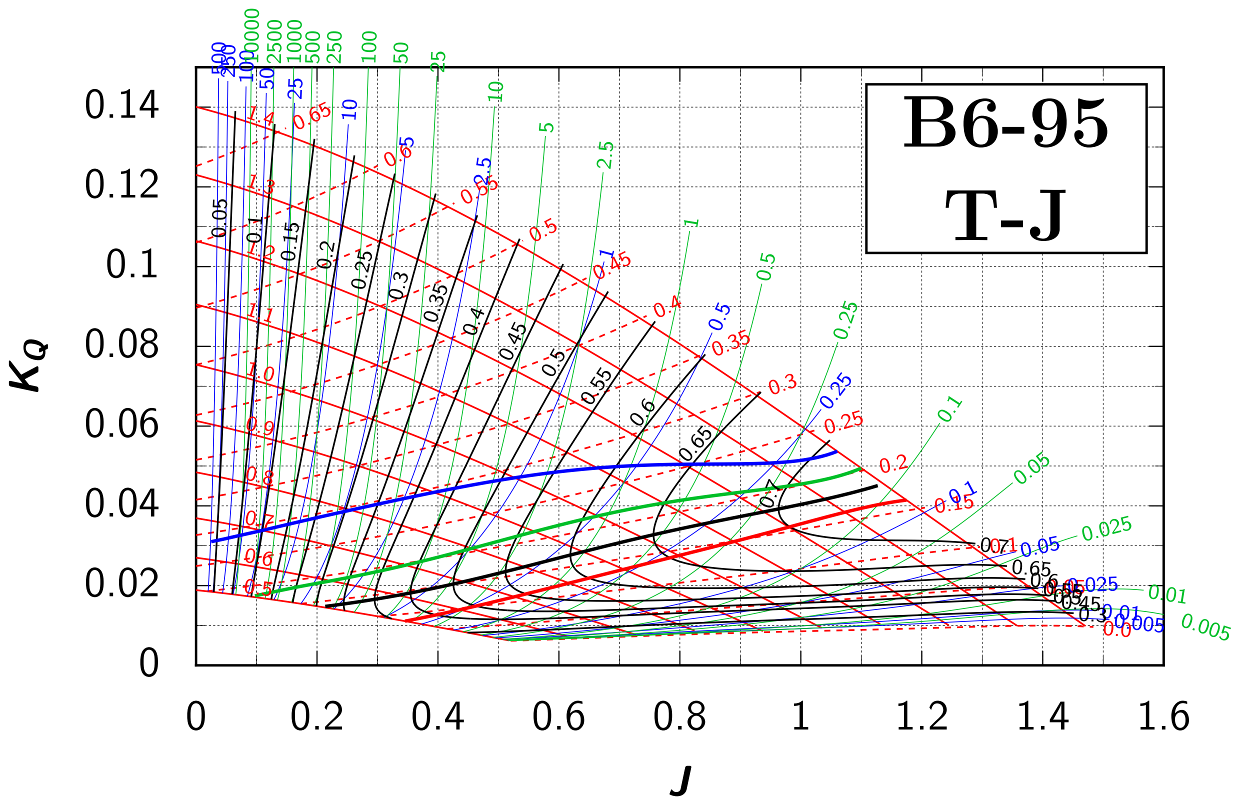

Preprints (www.preprints.org) | NOT PEER-REVIEWED | Posted: 10 December 2019 doi:10.20944/preprints201912.0140.v1

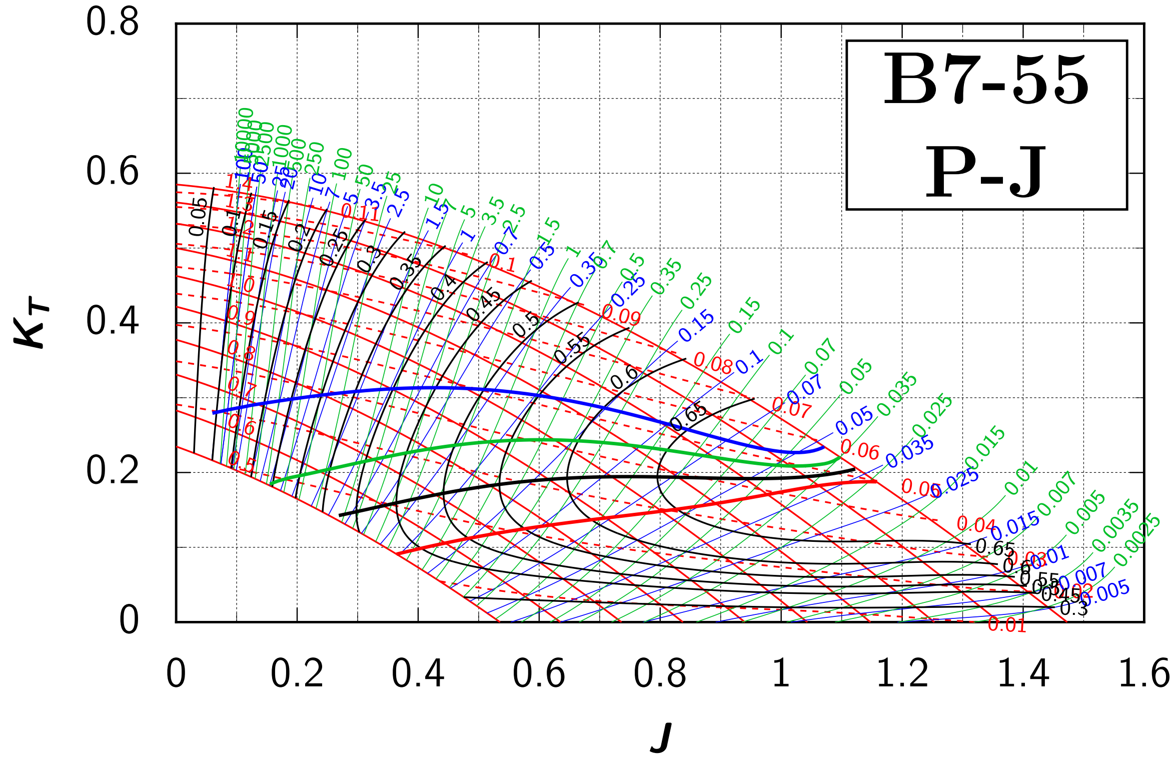

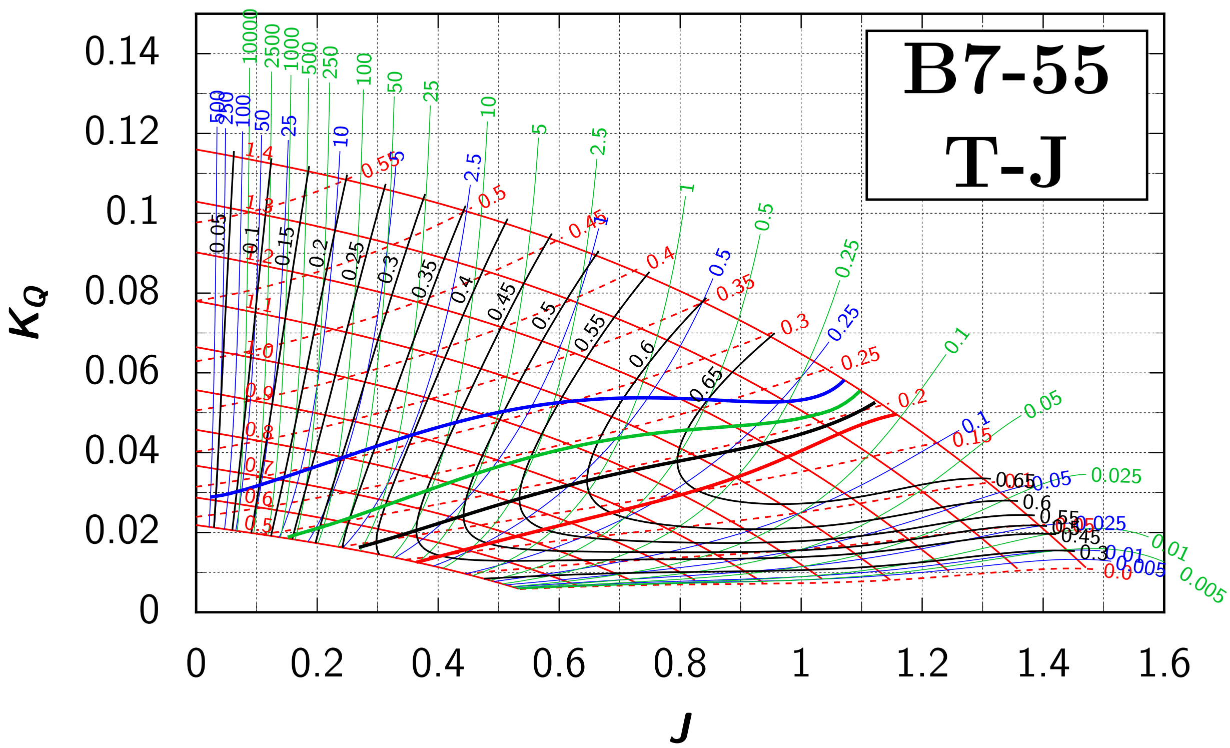

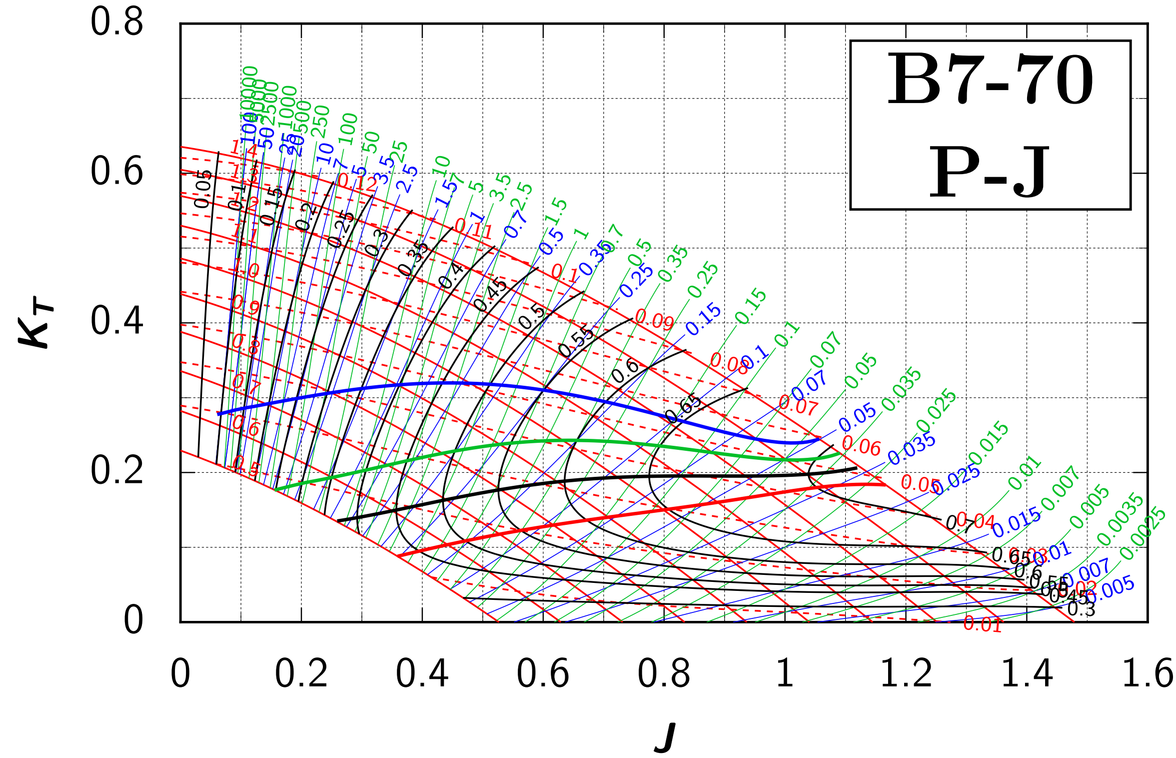
B7-70
P-J
K_T
J

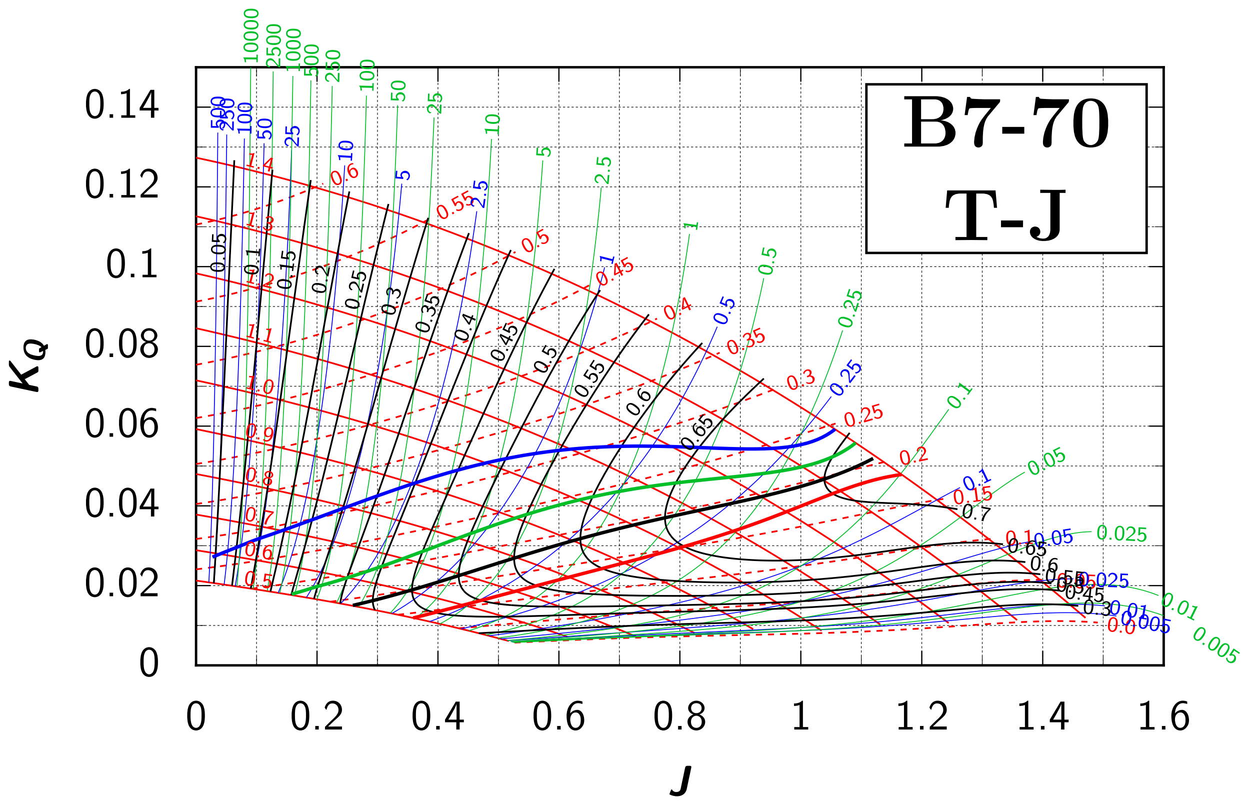
B7-70
T-J
K_Q
J

Preprints (www.preprints.org) | NOT PEER-REVIEWED | Posted: 10 December 2019 doi:10.20944/preprints201912.0140.v1

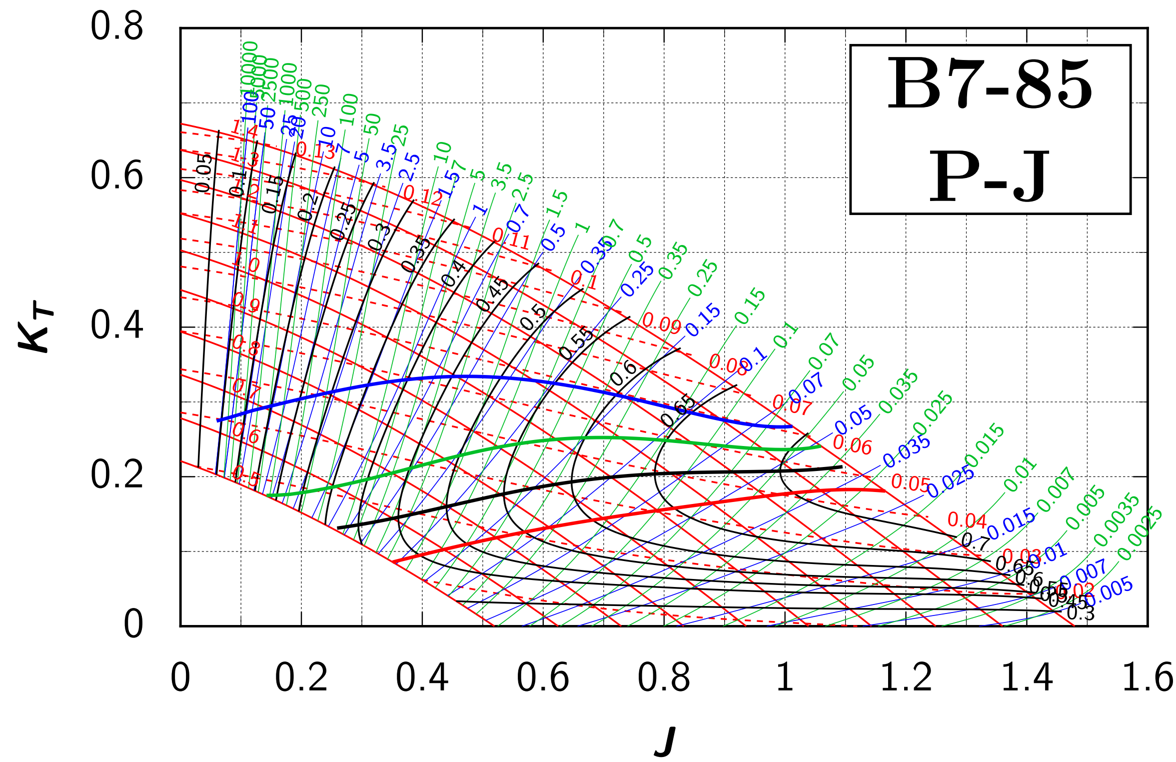

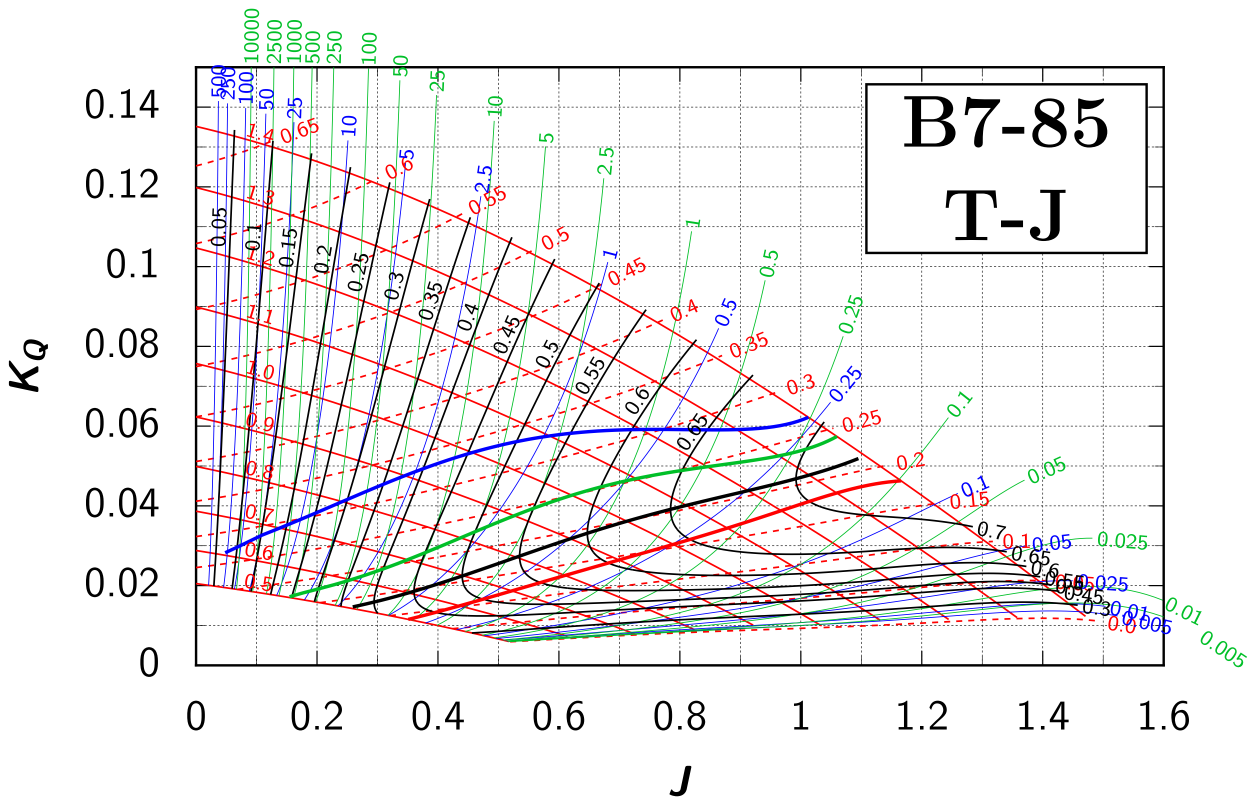

Preprints (www.preprints.org) | NOT PEER-REVIEWED | Posted: 10 December 2019 doi:10.20944/preprints201912.0140.v1

References

1. 28th ITTC Quality Systems Group. ITTC Symbols and Terminology List. **2017**, https://ittc.info/media/7937/structured-list_2017_a.pdf.
2. Bendemann, F. & Madelung, G. Praktische Schraubenberechnung, 15. Bericht der Deutschen Versuchsanstalt für Luftfahrt. *Technische Berichte der Flugzeugmeisterei* **1917**, *2*, 53–80
3. Danckwardt, E. Berechnungsdiagramme für Schiffsschrauben. *Schiffbautechnik* **1956**, *2*, 22–30.
4. Helma, S. Wageningen B-Series revisited. *The 5th International Conference on Advanced Model Measurement Technology for The Maritime Industry (AMT'17)*, **2017**. Strathclyde University, Glasgow, Scotland (UK).
5. Helma, S. Surprising behaviour of the Wageningen B-Series polynomials. *Sixth International Symposium on Marine Propulsors (smp'17)*, **2019**. Rome, Italy.
6. van Lammeren, W.P.A. & van Aken, J.A. Een Uitbreiding van de Systematische 3- en 4-bladige Schroefseries van het Nederlandsch Scheepsbouwkundig Proefstation. *N.S.M.B. Publication* **1949**, *78* (published in *Schip en Werf* 13, 264–281).
7. van Lammeren, W.P.A., van Manen, J.D. & Oosterveld, M.W.C. The Wageningen B-screw Series. *Trans. S.N.A.M.E.* **1969**, *77*, 269–317.
8. Oosterveld, M.W.C. & van Oossanen, P. Further Computer-Analysed Data of the Wageningen B-screw Series. *N.S.M.B. Publication* **1975** *479* (reprinted from *Int. Shipbuilding Progress* 22(251)).
9. Papmel, E.E. Practical design of the screw propeller (in Russion) Leningrad 1936 (cited from [13])
10. Schoenherr, K. Propulsion and propellers. In *Principles of Naval Architecture*; Rossell H.E., Chapman, L.B., Eds.; SNAME, New York, USA; 1949; pp. 158–168.
11. von der Steinen, C. Praktische Schraubendiagramme. *Werft-Reederei-Hafen* **1923**, *4*, 61–72
12. Yosifov, K.Y. & Staneva, A.D. Propeller Design Charts. *Bulgarian Ship Hydrodynamics Centre (BSHC)*, **1983**, Varna, Bulgaria.
13. Yosifov, K., Zlatev, Z., Staneva, A. Optimum Characteristics Equations for the 'K-J' Propeller Design Charts, based on the Wageningen B-screw Series. *Int. Shipbuilding Progress* **1986**, *33*(382), 101–111